British Journal of Pharmacology

British Journal of Pharmacology (2017) **174** 4277–4294 4277

RESEARCH PAPER

Selective targeting of M-type potassium $K_v7.4$ channels demonstrates their key role in the regulation of dopaminergic neuronal excitability and depression-like behaviour

Correspondence Hailin Zhang, Department of Pharmacology; The Key Laboratory of Neural and Vascular Biology, Ministry of Education; The Key Laboratory of New Drug Pharmacology and Toxicology, Hebei Medical University, Shijiazhuang, Hebei, China. E-mail: zhanghl@hebmu.edu.cn

Received 18 April 2017; **Revised** 20 August 2017; **Accepted** 21 August 2017

Li Li[1,*], Hui Sun[1,*], Jie Ding[1], Chenxu Niu[1], Min Su[1], Ludi Zhang[1], Yingmin Li[2], Chuan Wang[1], Nikita Gamper[1,3], Xiaona Du[1] and Hailin Zhang[1]

[1]*Department of Pharmacology; The Key Laboratory of Neural and Vascular Biology, Ministry of Education; The Key Laboratory of New Drug Pharmacology and Toxicology, Hebei Medical University, Shijiazhuang, Hebei, China,* [2]*Department of Forensic Medicine, Hebei Medical University, Shijiazhuang, Hebei, China, and* [3]*Faculty of Biological Sciences, University of Leeds, Leeds, UK*

*These authors contributed equally to this work.

BACKGROUND AND PURPOSE

The mesolimbic dopamine system originating in the ventral tegmental area (VTA) is involved in the development of depression, and firing patterns of VTA dopaminergic neurons are key determinants in this process. Here, we describe a crucial role for the M-type $K_v7.4$ channels in modulating excitability of VTA dopaminergic neurons and in the development of depressive behaviour in mice.

EXPERIMENTAL APPROACH

We used $K_v7.4$ channel knockout mice and a social defeat model of depression in combination with electrophysiological techniques (patch clamp recording and *in vivo* single-unit recordings), immunohistochemistry, single-cell PCR and behavioural analyses (social interaction time and glucose preference tests) to investigate VTA circuits involved in the development of depression-like behaviour.

KEY RESULTS

Among the K_v7 channels, $K_v7.4$ channels are selectively expressed in dopaminergic neurons of the VTA. Using a newly identified selective $K_v7.4$ channel activator, fasudil, and $K_v7.4$ channel knockout mice, we demonstrate that these channels are a dominant modulator of excitability of VTA dopaminergic neurons, *in vitro* and *in vivo*. Down-regulation of $K_v7.4$ channels could be a causal factor of the altered excitability of VTA dopaminergic neurons and depression-like behaviour. The selective $K_v7.4$ channel activator, fasudil, strongly alleviated depression-like behaviour in the social defeat mouse model of depression.

CONCLUSION AND IMPLICATIONS

Because expression of $K_v7.4$ channels in the CNS is limited, selectively targeting this M channel subunit is likely to produce less on-target side effects than non-selective M channel modulators. Thus, $K_v7.4$ channels may offer alternative targets in treatment of depression.

Abbreviations

ISI, interspike interval; SN, substantia nigra; SUS mice, susceptible mice; UNSUS mice, unsusceptible mice; VTA, ventral tegmental area

DOI:10.1111/bph.14026

Introduction

Current treatments available for major depression are unsatisfactory due to their many side effects and low efficacy, leaving more than one-third of depressed individuals resistant to drug treatments (Wong and Licinio, 2001). In addition, antidepressants usually take several weeks to months to produce a therapeutic response. Thus, new strategies are needed to understand the pathophysiology of major depression and to develop new therapeutic treatments. Growing evidence has implicated the mesolimbic **dopaminergic** system originating in the ventral tegmental area (VTA) in the pathogenesis and treatment of depression (Dunlop and Nemeroff, 2007; Gershon *et al.,* 2007; Krishnan *et al.,* 2007). The dopaminergic neurons of the VTA fire either tonically or in 'phasic' bursts, and these firing patterns were shown to encode different types of behaviour (Schultz, 2007). The phasic burst firing of VTA dopaminergic neurons is sufficient to drive behavioural conditioning and elicit dopaminergic transients with magnitudes not achieved by longer, lower-frequency spiking (Tsai *et al.,* 2009). More importantly, it has been recently demonstrated that the phasic burst firing pattern of VTA dopaminergic neurons directly controls depression-like behaviour in rodent models of depression (Chaudhury *et al.,* 2013; Tye *et al.,* 2013).

A key to understanding the molecular and cellular mechanisms underlying depression lies in deciphering the firing patterns of dopaminergic neurons in the VTA and identification of the main molecular players controlling such patterns (Grace *et al.,* 2007). Ionotropic **NMDA receptors** and Ca^{2+}-activated K^+ channels (Creed *et al.,* 2016), **HCN** (Neuhoff *et al.,* 2002; Cao *et al.,* 2010) and **$K_{ir}3$/GIRK** channels (Munoz and Slesinger, 2004; Padgett *et al.,* 2012) have all been suggested to play important roles in controlling either the intrinsic dopaminergic neuronal activity or the abusive drug-induced modulation of such activity. However, despite significant progress, a complete understanding of the firing patterns within the VTA circuitry and what controls these patterns is currently lacking. One emerging concept for treating depression is focused on modulation of the **K^+ channels** of VTA dopaminergic neurons (Overstreet and Wegener, 2013; Borsotto *et al.,* 2015). This concept is based on several experimental findings suggesting that K^+ channels controlling excitability of VTA dopaminergic neurons may be targeted to reduce the neuronal firing and the susceptibility of mice to social depression stress (Krishnan *et al.,* 2007; Friedman *et al.,* 2014; Friedman *et al.,* 2016). Several other studies have implicated K^+ channels in depression (even though some of these observations are not directly compatible); thus, genetic deletion of **TREK1 K^+ channels** produces an intrinsic antidepressant-like phenotype, which is not affected by further treatment with SSRI antidepressants (Heurteaux *et al.,* 2006), while selective blockade of TREK1 channels with spadin or its analogues exerts a rapid antidepressant effect (Mazella *et al.,* 2010; Veyssiere *et al.,* 2015).

One family of K^+ channels, which is increasingly recognized for their role in controlling neuronal firing, is the K_v7/KCNQ family. K_v7/KCNQ channels ($K_v7.1$–5) are voltage-dependent potassium channels with five members, four of which (**$K_v7.2$**–5) are abundantly expressed in the CNS (Wang *et al.,* 1998; Jentsch, 2000; Gamper and Shapiro, 2015). Opening of K_v7 channels leads to neuronal hyperpolarization, membrane potential stabilization and decreased excitability. This makes these K^+ channels particularly interesting as targets in neurological disorders linked to hyperexcitability, including epilepsy, anxiety, pain, migraine and addiction to psychostimulants (Brown and Passmore, 2009). Interestingly, K_v7 channels are expressed in dopaminergic neurons (Hansen *et al.,* 2006; Koyama and Appel, 2006) and have been suggested to modulate the excitability of dopaminergic neurons (Hansen *et al.,* 2008; Drion *et al.,* 2010) and dopaminergic transmission (Hansen *et al.,* 2008). On the transcriptional level, **$K_v7.4$** channels were found to be a major KCNQ gene expressed in VTA dopaminergic neurons (Hansen *et al.,* 2006), although the functional expression and potential role of K_v7 channels in depression have not been elucidated. In this study, we provide strong evidence that $K_v7.4$ channels are a dominant subtype of K_v7 channels in the VTA and potent modulators of the excitability of VTA dopaminergic neurons. Because the expression of $K_v7.4$ channels in the CNS is much more restricted than the expression of other K_v7 channels, targeting this channel may offer a new approach to the treatment of depression, and such a strategy could be less prone to on-target side effects than current treatments.

Methods

Animals

All animal care and experimental procedures were conducted in accordance with the guidelines and with the approval of the Animal Care and Use Committee at Hebei Medical University. Animal studies are reported in compliance with the ARRIVE guidelines (Kilkenny *et al.,* 2010; McGrath and Lilley, 2015).

Animals were housed in conditions of controlled temperature, humidity and lighting (12:12 h light–dark cycle) and given free access to food (provided by Experimental Animal Center of Hebei Province) and tap water *ad libitum*. Animals were allowed to adapt to their housing environment for at least 7 days prior to experimentation and to the experimental room for 1 day before experiments. $K_v7.4$ knockout mice ($K_v7.4^{-/-}$) were kindly provided by Prof Thomas Jentsch (FMP, MDC, Berlin, Germany) (Kharkovets *et al.*, 2006). A total of 321 male wild-type (WT) and 210 male $K_v7.4^{-/-}$ C57BL/6 J mice (7–8 weeks old, Vital River, China) were used for the studies.

Cell culture

CHO K1 cells stably expressing $K_v7.4$ or $K_v7.2$/**7.3** channels were maintained in F12 media (Life Technologies, USA) supplemented with 10% fetal calf serum, non-essential amino acid supplement (Gibco, USA), 600 $\mu g \cdot mL^{-1}$ G418 and 600 $\mu g \cdot mL^{-1}$ hygromycin B and incubated at 37°C in 5% CO_2. CHO K1 cells transiently transfected with $K_v7.2$ were grown in F12 supplemented with 10% fetal calf serum and 1% penicillin–streptomycin. Cells were grown on glass coverslips and transfected using Lipofectamine (Life Technologies, USA). Recordings were performed 24–48 h after

transfection. Human $K_v7.2$, rat **$K_v7.3$** and human $K_v7.4$ (GenBank accession numbers: AF110020, AF091247, AF105202, respectively) were kindly provided by Diomedes E. Logothetis (Virginia Commonwealth University, Richmond, Virginia, USA) and were subcloned into pcDNA3.

VTA brain slice preparation

Brain slices containing VTA/substantia nigra (SN) were prepared as reported (Krishnan *et al.,* 2007). Mice were killed by pentobarbital sodium (200 $mg \cdot kg^{-1}$, i.p), and brains were cut in a coronal plane and sectioned into slices (250μm) containing VTA/SN using a vibratome (VT1200S; Leica, Germany). The VTA was located stereotaxically, as described (Franklin and Paxinos, 2001), as the region dorsal to the medial mammillary nucleus or the interpeduncular nucleus, medial to the SN and ventral to the red nucleus (Shabat-Simon *et al.,* 2008). The coronal slices (250 μm) were prepared in ice-cold oxygenated (95% O_2/5% CO_2) cutting solution (in mM: KCl 2.5, NaH_2PO_4 1.25, $NaHCO_3$ 25, $CaCl_2$ 0.5, $MgCl_2$ 7, D-glucose 10 and sucrose 220; osmolarity, 295–305 mOsm) and incubated for 30 min at 36°C in oxygenated artificial CSF (aCSF) (in mM: NaCl 124, KCl 3, NaH_2PO_4 1.24, $MgCl_2$ 2, $CaCl_2$ 2, D-glucose 10 and $NaHCO_3$ 26; osmolarity, 280–300 mOsm). Four coronal slices (250 μm) containing the VTA/SN were obtained from each mouse. The slices were allowed to recover at room temperature (23–25°C) in oxygenated aCSF for at least 1 h prior to recording. Recordings were made at room temperature in a recording chamber continuously perfused with oxygenated aCSF (2 $mL \cdot min^{-1}$).

The human brainstem from a 45-year-old male who died of sudden cardiac death without neuropsychiatric, neurological or neurodegenerative disease was obtained from the Department of Forensic pathology of Hebei Medical University. The use of human tissue samples was approved by the Ethical Committee for Human Tissue Samples of Hebei Medical University.

Identificationof VTA dopaminergic neurons

Dopaminergic neurons were distinguished from non-dopaminergic neurons either by the presence of tyrosine hydoxylase (TH), using single-cell PCR, or based on the functional characteristics of dopaminergic neurons as follows: (i) a sag hyperpolarization potential during injection of a hyperpolarizing current pulse (Supporting Information Figure S1A, B); (ii) a typical triphasic action potential with a negative deflection, an action potential width from the start to the minimum of >1.1 ms and an action potential duration (from start to recovery at resting membrane rest) > 2.5 ms (Supporting Information Figure S1C, D); (iii) firing rate less than 5 Hz (in loose patch or single-unit recordings where spontaneous firing was recorded; see below); and (iv) inhibition of the firing activity by dopamine (Ungless *et al.,* 2004; Cao *et al.,* 2010).

Electrophysiology

K_v7 channel current recordings in CHO cells expressing these channels were made using the perforated patch configuration of the patch-clamp technique (amphotericin B, 250 $\mu g \cdot mL^{-1}$, Sigma, USA) at room temperature using a HEKA EPC10 patch-clamp amplifier and Patch Master software (HEKA Electronics, Germany). Currents were acquired at 10 kHz and filtered at 2.5 kHz. Patch electrodes were pulled with a micropipette puller (Sutter Instruments, USA) and polished to 2–4 MΩ resistance. The intracellular solution contained the following (in mM): KCl 150, $MgCl_2$ 5, HEPES 10, pH adjusted to 7.4 with KOH. Series resistance (generally below 10 MΩ) was compensated by 60–80%. The extracellular solution contained (in mM) the following: NaCl 160, KCl 2.5, $MgCl_2$ 1, $CaCl_2$ 2, glucose 10, HEPES 20; pH adjusted to 7.4 with NaOH. Cells were held at a holding potential of −60 mV, and 1 s test pulses to −10 mV were applied every 6 s.

For whole-cell current-clamp and voltage-clamp recordings in the VTA slices, an Axopatch 1D amplifier coupled with a Digidata 1440A AD converter (Molecular Devices, USA) was used, and the data were analysed using Clampex 10.3 (Molecular Device, USA) and OriginPro 8.5 software (Origin Lab Corporation, USA). For K_v7 channel/M current recordings, neurons were held at −10 mV and 1 s square pulses to −50 mV were delivered repeatedly at 20 s intervals. The M current was measured as the instantaneous deactivating tail current at the beginning of a voltage step to −50 mV. Whole-cell patch-clamp recordings were made with glass electrodes (4–6 MΩ) using an internal solution containing (in mM): K-methylsulfate 115, KCl 20, $MgCl_2$ 1, HEPES 10, EGTA 0.1, MgATP 2 and Na_2GTP 0.3, pH adjusted to 7.4 with KOH. The extracellular solution was the aCSF. A cell-attached 'loose-patch' (100–300 MΩ) (Burlet *et al.,* 2002) recordings were also used to record spontaneous firing of dopaminergic neurons. In this case, the pipette solution contained aCSF.

Single-unit recordings were used to record the spontaneous firing of VTA dopaminergic neurons *in vivo* based on a previously reported method (Mameli-Engvall *et al.,* 2006). Briefly, mice were anaesthetized with 4% chloral hydrate (400 $mg \cdot kg^{-1}$, i.p.); the coordinates for the VTA were 2.92–3.16 mm from the anterior fontanel, 0.50–0.70 mm lateral from the midline and 4.20–5.00 mm ventral from the cortical surface. Dopaminergic neurons were identified by their characteristic action potentials [typical triphasic action potentials with a negative deflection: the action potential width from the start to the minimum trough of ≥1.1 ms, a characteristic long duration (>2 ms) and a slow firing rate (<10 Hz)] (Cao *et al.,* 2010) (Figure 3F). The presence of burst firing (as opposed to tonic firing) was identified by the following criteria: (i) the start of a burst was registered when two consecutive spikes fired within 80 ms; (ii) the end of the burst was registered when the interspike interval (ISI) exceeded 160 ms (Cao *et al.,* 2010); and (iii) a neuron was considered as burst-firing if it fired at least one burst within 3 min. Electrical signals were amplified and filtered (10-4 K Hz) by the Axoclamp 900A preamplifier and recorder by the Digidata 1440A AD converter (Molecular Devices, USA); the data were analysed by Clampfit 10.3 (Molecular Devices, USA).

The effect of 0.9% saline (vehicle), **fasudil** (20 $mg \cdot kg^{-1}$) or **retigabine** (10 $mg \cdot kg^{-1}$) on the firing activity of VTA dopaminergic neurons recorded using single-unit recordings was assessed 10 min after i.p. injection or 5 min after direct VTA local pressure (5–15 ψ) injection (see Figure 6 legend for detail). The effects of drugs on the following parameters were analysed: (i) average firing rates (Hz); (ii) corresponding

ISI (ISI histograms were plotted for at least 5 min of continuous recording); (iii) percentage of cells displaying burst firing (number of burst firing cells/number of all cells recorded × 100%); (iv) average number of spikes in a burst (number of spikes in burst/number of burst events); and (v) percentage of spikes in bursts (number of spikes in bursts/total number of spikes × 100%).

Chronic social defeat stress

The social defeat model of depression in mice was established based on the protocols reported previously (Krishnan *et al.*, 2007). Briefly, the C57BL/6 mice were subjected to attack by a CD1 mouse for 10 min a day for 10 days. CD1 retired breeders were selected before the test and the fiercest CD1 mice were excluded in the following experiment. In addition, the intensity of attack stimuli was minimized to produce stable depressive behaviour. To minimize harm and avoid physical injury, plastic dividers were set when C57BL/6 J mice displayed submissive behaviour, including immobility, crouching, trembling, fleeing and upright posture. On day 1 and day 11, the weight was recorded, and a sucrose preference test was performed as follows. Mice were individually accommodated in cages with two drinking water bottles for 24 h (food provided *ad libitum*). The animals were then deprived of water and food for 12 h. After this period, two drinking bottles were re-introduced with one containing 0.8% sucrose solution and the other filled with drinking water. Twelve hours later, the bottles were removed and weighed. Sucrose preference was calculated as a percentage [(weight of sucrose solution consumed / total weight of liquid consumed from two bottles) × 100%]. On day 13, the social interaction test was carried out. The C57BL/6 mice were placed in an interaction test box and allowed to move freely for 2.5 min in the absence or presence of an unfamiliar caged CD1 mouse. The time the test C57BL/6 mice spent in the interaction zone and in the corner zone (see Supporting Information Figure S2A, B) was analysed (Supporting Information Figure S2C). Subgroups of susceptible (SUS) and unsusceptible (UNSUS) mice were identified. The animals were qualified as SUS to depression-like behaviour (SUS) if they spent significantly less time in the interaction zone while a CD1 mouse was present than while a CD1 mouse was not present. Animals that did not respond to the presence of a CD1 mouse by reduced interaction time were qualified as UNSUS mice. Sucrose preference was an additional test used to determine depression susceptibility (see below). Animals were divided into groups randomly. Experimenters were blinded to the drug treatment while performing the tests.

Cannula implantation for direct injection of drugs into the VTA

Mice were anaesthetized by i.p. injection of 8% chloral hydrate (400 mg·kg^{-1}, i.p) and placed into a stereotaxic apparatus. Mice were bilaterally implanted with a stainless 26-gauge cannula fitted with obturators (Plastics One) targeting directly above the VTA with the following coordinates: anteroposterior, 3.08 mm; lateral, 0.50 mm; and dorsoventral, 4.20 mm. The cannulae were secured with dental cement; and the mice were then singly housed and allowed to recover for 3 days. After the surgery, the mice were housed at 28°C for 8 h to maintain their body temperature. All instruments were autoclaved, and the skin of the animals was sterilized with alcohol and iodine to prevent infection after surgery. The animals were placed in a cage with clean sawdust bedding and provided free access to fresh water and food (provided by the Experimental Animal Center of Hebei Province).

Western blotting

Mice were killed by pentobarbital sodium (200 mg·kg^{-1}, i.p) and perfused transcardially with 0.01 m ice-cold PBS. Brains were rapidly removed, and VTA punches (2 mm diameter, 2 mm thick) from these mice were sonicated in 1% SDS lysis buffer containing protease inhibitor and centrifuged at 4°C for 30 min at 17 220 g. Protein samples (40 mg) were separated by 10% SDS-PAGE for 1.5 h and transferred to a nitrocellulose membrane for 2 h in 20% transfer buffer. Membranes were then blocked for 1 h at room temperature in TBST (TBS and 0.1% Tween-20) with 5% non-fat milk (Sigma, USA) and then were incubated overnight at 4°C with primary antibody against K_v7.4 channel protein (1:1000, Alomone Labs, USA) or β-tubulin (1:10 000, Abcam, UK) diluted in TBST. Membranes were washed with TBST for 3 × 10 min, incubated with goat anti-rabbit (1:5000, Rockland, USA) or goat anti-mouse (1:7500, Rockland, USA) secondary antibodies for 1 h at room temperature and washed with TBST for 2 × 10 min followed by another 10 min wash with TBS. Membranes were imaged using an Odyssey infrared imaging system (LI-COR, USA); the integrated optical density of each band was measured using ImageJ software (National Institutes of Health, USA).

Immunofluorescence

For experiments shown in Figure 1D, mice were killed by pentobarbital sodium (200 mg·kg^{-1}, i.p.) and perfused transcardially with 0.01 m ice-cold PBS, followed by ice-cold PBS containing 4% paraformaldehyde (PFA). The brain was removed, fixed in 4% PFA at 4°C for 48 h and embedded in paraffin. Paraffin coronal VTA/SN slices (5 μm) were mounted on glass slides. Coronal VTA/SN slices located at 1.40 to 0.50 mm from λ. Slices were dewaxed in xylene and rehydrated in alcohol. Antigen retrieval was achieved by microwave heating (three times for 3 min) of the brain slices. Sections were blocked with 10% goat serum (Biological Industries, Israel) in PBS and incubated overnight with a mixture of mouse anti-TH (1:100, Merck Millipore, Germany, Cat# MAB318 Lot#, RRID: AB_2201528) and rabbit anti-K_v7.4 (1:100, AlomoneLabs, Israel, Cat# APC-164 Lot#, RRID: AB_2341042) antibodies. Sections were then washed with PBS six times (5 min) and incubated in FITC-conjugated AffiniPure goat anti-mouse IgG (Jackson ImmunoResearch, USA, Labs Cat# 115–095-003, RRID:AB_2338589; 1:200) and Cy3-conjugated AffiniPure goat anti-rabbit IgG (Jackson ImmunoResearch, USA; 1:200, Labs Cat# 111–165-003, RRID:AB_2338000) for 30 min at 37°C. Sections were then washed six times (5 min) with PBS. Subsequently, sections were counterstained with DAPI (Sigma, USA) to identify nuclei for 20 min at room temperature and washed three times with PBS (5 min). Finally, slices were mounted with Prolong Gold antifade reagent (Life Technologies, USA).

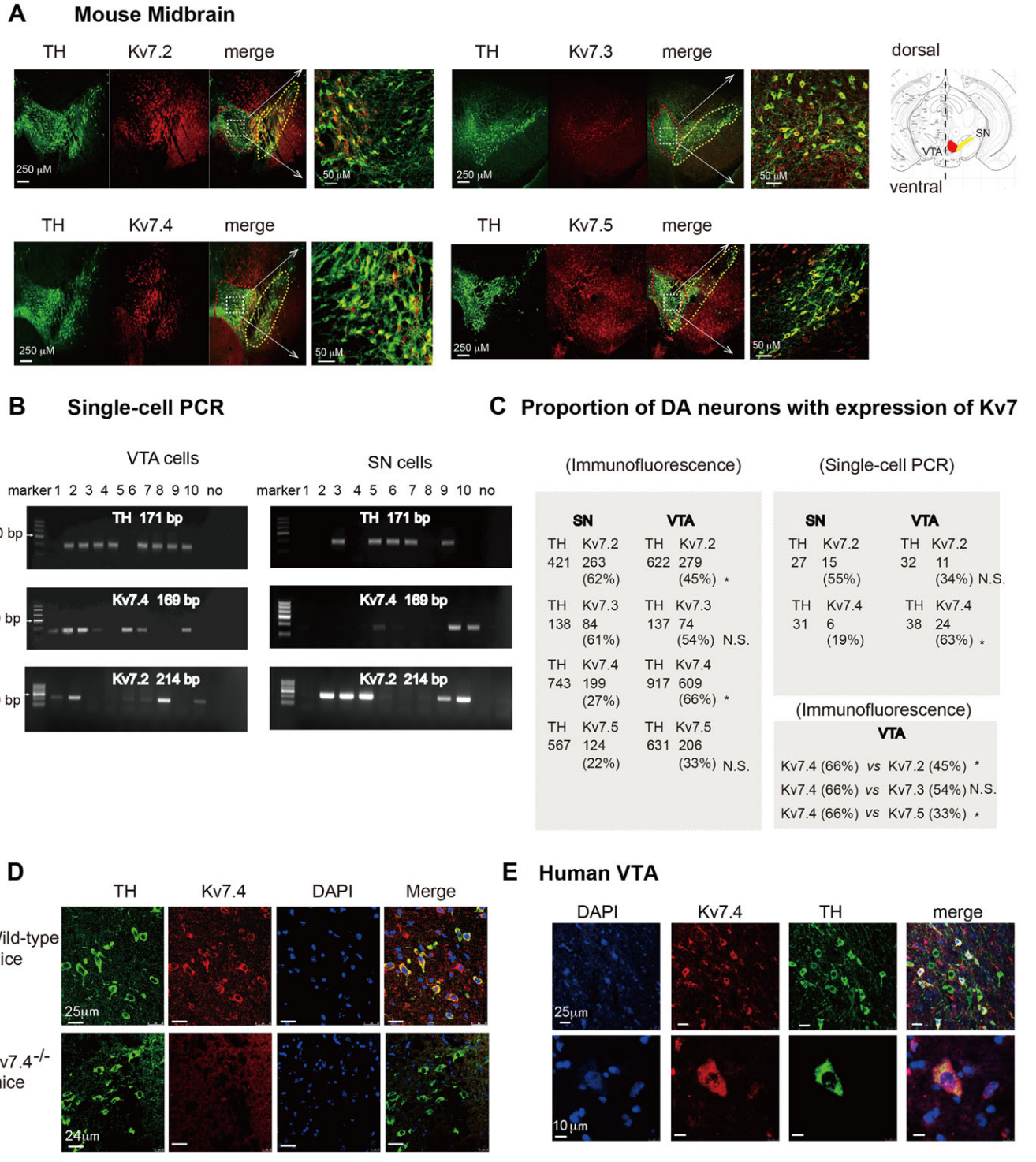

Figure 1

The expression of K_v7 channels in the midbrain. (A) Representative immunofluorescence images of the co-expression of K_v7 subtypes ($K_v7.2$, $K_v7.3$, $K_v7.4$ and $K_v7.5$) and tyrosine hydroxylase (TH) in the mesencephalon of the mice. The VTA and SN are highlighted by the red and yellow dotted circles, respectively, and a zoomed-in area of the VTA is shown by the dotted square and the white arrows. A schematic of the VTA (red) and SN (yellow) areas in the map of a midbrain coronal section is also shown in the inset on the right. (B) RT-PCR analysis of single neurons from VTA and SN brain slices. The lane numbers correspond to individual neurons; 'no' denotes the negative control in which no template (neuronal lysate) was added in the RT-PCR reaction. The expected sizes of the DNA products for TH and K_v7 channels are shown. (C) Proportions of dopaminergic (DA) neurons (TH-positive) expressing individual K_v7 subtypes, analysed for protein (immunofluorescence) and mRNA (single cell PCR) levels. (D) Immunofluorescent identification of $K_v7.4$ (red) and TH (green) expression in the VTA of WT and $K_v7.4$ knockout ($K_v7.4^{-/-}$) mice. (E) $K_v7.4$ (red) and TH (green) in a VTA slice from human brain.

For experiments shown in Figure 1A, the brain was fixed in 4% PFA at 4°C for 24 h and embedded in 30% sucrose for 24 h. Coronal VTA/SN slices (60 μm) were cut using a vibratome (VT1200S; Leica, Germany). Sections were blocked with 10% goat serum overnight with a mixture of two primary antibodies: mouse anti-TH (1:100, Merck Millipore, Germany) and rabbit anti-K_v7.2 (1:100, Santa Cruz, CA, Cat# sc-7793, RRID: AB_2296585), goat anti-K_v7.3 (1:100, Santa Cruz, CA, Cat# sc-7794 Lot#, RRID: AB_2131714), rabbit anti-K_v7.4 (1:100, AlomoneLabs, Israel) or rabbit anti-K_v7.5 (1:50, Santa Cruz, CA, Cat# sc-50416 Lot#, RRID: AB_2131834). Sections were then washed with PBS six times (5 min) and incubated in a mixture of two secondary antibodies: FITC-conjugated AffiniPure goat anti-mouse IgG (Jackson ImmunoResearch, USA; 1:200) and Cy3-conjugated AffiniPure goat anti-rabbit IgG (Jackson ImmunoResearch, USA; 1:200) for 30 min at 37°C. Sections incubated with anti-K_v7.3 antibody were incubated in Cy5-conjugated AffiniPure donkey anti-goat IgG (Jackson ImmunoResearch, USA, Labs Cat# 705–175-147, RRID:AB_2340415; 1:400) and FITC-conjugated AffiniPure donkey anti-mouse IgG (Jackson ImmunoResearch, USA, Labs Cat# 715–095-151, RRID: AB_2335588; 1:400).

Images were taken using a Leica TCS SP5 confocal microscope (Leica, Germany) equipped with laser lines for DAPI (800 nm, Ti-sapphire coherent pulsed), FITC (Argon 488), cy3 (HeNe 543) and cy5 (red diode 637 nm). Images were analysed with LAS-AF-Lite software (Leica).

Tissue blocks of the brainstem from human brain were fixed in 4% PFA at 4°C and embedded in paraffin. Slices were dewaxed and rehydrated. Antigen retrieval and incubation with antibodies were performed by the same protocol used for mouse samples.

Single-cell PCR

Neurons were aspirated into a patch pipette at the end of electrophysiological recordings. The electrode tip was then broken into a PCR tube containing 1 μL of oligo-dT (50 mM) and 1 μL of dNTP mixture (10 mM). The mixture was heated to 65°C for 5 min to denature the nucleic acids and then placed on ice for 1 min. Single-strand cDNA was synthesized from the cellular mRNA by mixing 2 μL of 5× PrimeScript II buffer (50 mM), 0.5 μL of RNase inhibitor (40 U·μL^{-1}) and 1 μL of PrimeScript II RTase (200 U·μL^{-1}) and then incubating the mixture at 50°C for 50 min. Synthesis of single-cell cDNA was performed using a C1000 Touch thermal cycler-CFX96 Real-time PCR system (California, USA). First-strand synthesis was executed at 95°C (5 min) followed by 35 cycles (95°C for 1 min, 56°C for 45 s, 72°C for 50 s) and a final 10 min elongation at 72°C by adding the specific 'outer' primer pairs to each PCR tube (final volume 25 μL). Then, 2 μL of the product of the first PCR was used in the second amplification round by using the specific 'inner' primer (final volume 50 μL). The second amplification round consisted of heating the samples to 95°C for 5 min followed by 30 cycles (95°C for 1 min, 54–62°C for 45 s, 72°C for 50 s) and 10 min elongation at 72°C. The products of the second round of PCR were analysed in 2.5% agarose gels and stained with ethidium bromide. A PrimeScriptTM II 1 st Strand cDNA Synthesis Kit and GoTaq Green Master Mix were obtained from Takara-Clontech (Kyoto, Japan) and Promega (Madison, USA) respectively.

The 'outer' primers (from 5′ to 3′) are as follows:

GAPDH	AAATGGTGAAG GTCGGTGTGA ACG (sense)	AGTGATGGCATGGACT GTGGTCAT (antisense)
TH	ATACAAGCAGG GTGAGCCAA	TACACCGGCTGGTA GGTTTG
K_v7.2	TCTCCTGCCTT GTGCTTTCT	GCATCTGCGTAGGT GTCAAA
K_v7.4	CCCGGGTGGAC CAAATTGT	AGCCCTTCAGTCCA TGTTGG

The 'inner' primers (from 5′ to 3′) are as follows:

GAPDH	GCAAATTCAACGGC ACAGTCAAGG	TCTCGTGGTTCACA CCCATCACAA
TH	TTCTTGAAGGAACG GACTGGC	TCAGCCAACATGGG TACGTG
K_v7.2	AGGAAGCCGTTCTG TGTGAT	GCAGAGGAAGCCAA TGTACC
K_v7.4	ATGGGGCGCGT AGTCAAGGT	GGGCTGTGGTAGTC CGAGGTG

qRT-PCR

Total RNA from the VTA of mice was extracted using a mirVana miRNA Isolation Kit (Invitrogen, USA) according to the manufacturer's recommendations. The RNA was reverse transcribed into cDNA using a PrimeScript™ RT reagent kit with gDNA Eraser (TAKARA, RR047A, Japan). qRT-PCR of Kv7.4 and GAPDH was performed using an ABI PRISM 7300 Sequence Detection System (Applied Biosystems, USA) with a SYBR® Premix Ex Taq™ II (TliRNaseH Plus) kit (TAKARA, RR820A, Japan). The relative amounts of transcripts were normalized to GAPDH; the relative RNA expression levels were calculated using the following equation: relative gene expression = $2^{-(\triangle Ct\ sample\ -\ \triangle Ct\ control)}$. The following primers were used.

K_v7.4	5′- ATGGGGCGCGTAGTCAAGG T-3′ (sense);
	5′- GGGCTGTGGTAGTCCGAGGTG -3′ (antisense);
GAPDH	5′- GGTGAAGGTCGGTGTGAACG -3′ (sense);
	5′- CTCGCTCCTGGAAGATGGTG -3′ (antisense).

Data and statistical analysis

The data and statistical analysis comply with the recommendations on experimental design and analysis in pharmacology (Curtis *et al.*, 2015). Sample size was determined through power analysis using preliminary data obtained in our laboratory with the following assumptions: 'α' of 0.05 (two-tailed) and power of 90%. Data are reported as the means ± SEM. Statistical analysis of differences between groups was carried out by Student's paired or unpaired *t*-tests, as appropriate. For data that failed a normality test, a paired sample Wilcoxon signed rank test or Mann–Whitney tests was used. Multiple groups were compared using one-way ANOVA with Bonferronni's correction or by Kruskal–Wallis

ANOVA with a Mann–Whitney test. P values ≤0.05 were accepted as significant. Fisher's exact test was used to compare population size. Data analysis was carried out using OriginPro 9.1 (OriginLab Corp., Northampton, MA).

Materials

Retigabine and **Y-27632** were from Sigma-Aldrich (China). Fasudil was from the National Institute for the Control of Pharmaceutical and Biological Products (Beijing, China). **XE991** dihydrochloride was from Alomone Labs (Jerusalem, Israel). RL-648_81 (Kumar *et al.*, 2016) was synthesized by the Department of New Drugs Development, School of Pharmacy, Hebei Medical University. All solutions were prepared freshly on the test day.

Nomenclature of targets and ligands

Key protein targets and ligands in this article are hyperlinked to corresponding entries in http://www.guidetopharmacology.org, the common portal for data from the IUPHAR/BPS Guide to PHARMACOLOGY (Southan *et al.*, 2016), and are permanently archived in the Concise Guide to PHARMACOLOGY 2015/16 (Alexander *et al.*, 2015a,b,c).

Results

$K_v7.4$ channels are selectively expressed in VTA DA neurons

Among the K_v7/KCNQ isoforms, $K_v7.4$ is the predominant KCNQ gene transcript present in the midbrain VTA (Hansen *et al.*, 2006). We first performed detailed analysis of protein and mRNA expression of K_v7/KCNQ isoforms in the midbrain of mice, with a special interest in the expression of these K_v7 channels in dopaminergic neurons (identified by the expression of TH). In the immunofluorescence study (Figure 1A, C), $K_v7.2$–$K_v7.5$ channels were differentially expressed in the dopaminergic neurons of the VTA and the SN of the mouse midbrain. Overall, among the four K_v7 isoforms, $K_v7.4$ was more selectively expressed in VTA than in the dopaminergic neurons of the SN. Thus, while 66% of TH-positive (dopaminergic) neurons in the VTA expressed $K_v7.4$ channels, only 27% of these neurons in the SN expressed this channel ($P < 0.05$; Fisher's exact test). Among the other K_v7 channels, only $K_v7.5$ exhibited a (non-significant) trend towards a higher incidence of expression in the VTA, compared to the SN (Figure 1C), yet the proportion of $K_v7.5$-positive neurons in the VTA was still significantly lower compared to the proportion of $K_v7.4$-positive neurons (Figure 1C). Interestingly, $K_v7.2$ channels were significantly more frequently expressed in SN neurons compared to VTA neurons (Figure 1C). $K_v7.3$ and $K_v7.5$ channels were expressed in much smaller proportions of VTA dopaminergic neurons (Figure 1C).

Similarly, in a single-cell PCR study (Figure 1B, C), $K_v7.4$ channels were also more selectively expressed in VTA dopaminergic neurons, with a trend towards more $K_v7.2$ channels in SN dopaminergic neurons (Figure 1C). $K_v7.4$ channels were absent from the VTA dopaminergic neurons of the $K_v7.4$ knockout mice ($K_v7.4^{-/-}$) ; Figure 1D). Expression of $K_v7.4$ channels was also found in human VTA dopaminergic neurons (Figure 1E). Taken together, the results presented in Figure 1 demonstrate that, while several K_v7 channels are expressed in VTA dopaminergic neurons, the $K_v7.4$ channels are predominant.

Fasudil selectively activates $K_v7.4$ currents in VTA dopaminergic neurons

We next aimed to selectively modulate $K_v7.4$ channels to regulate the excitability of VTA dopaminergic neurons. Our first goal was to identify a selective modulator of $K_v7.4$ channels. In a separate investigation of the effects of Rho-associated protein kinase (ROCK; Uehata *et al.*, 1997) inhibitor fasudil in the cardiovascular system, we discovered that fasudil is also a selective opener of $K_v7.4$ channels (Zhang *et al.*, 2016). Here, in CHO cells that exogenously express $K_v7.4$ channels, fasudil enhanced $K_v7.4$ channel currents, in a concentration-dependent manner, but did not affect currents carried by $K_v7.2$ channels (Supporting Information Figure 2A1–A3). Retigabine, a prototypic, non-selective, opener of K_v7 channels (Tatulian *et al.*, 2001), enhanced both $K_v7.4$ and $K_v7.2$ channel currents, which were inhibited by the K_v7 channel blocker XE991 (Supporting Information Figure 2A1, A2). Importantly, fasudil did not activate heterologously expressed $K_v7.2$/$K_v7.3$ multimeric channels (Supporting Information Figure S3), which are the major carriers of the M-type current in the CNS (Wang *et al.*, 1998). Fasudil did not affect $K_v7.1$ and $K_v7.3$ channels but did activate $K_v7.4$/$K_v7.5$ multimers (Zhang *et al.*, 2016). Thus, we concluded that fasudil is a selective activator of $K_v7.4$-containing homo- and heteromeric K_v7 channels.

We then tested the effect of fasudil on K^+ currents in VTA neurons. We recorded K_v7/M-like currents from VTA/SN slices of adult mice (6–8 weeks). The currents were recorded using the protocol shown in the right panel of Figure 2B1 as the characteristic slow deactivating tail current at −50 mV, which is defined as the 'M current' and is mostly conducted by K_v7 channels (Koyama and Appel, 2006). Accordingly, almost 50% of the deactivating current was inhibited by XE911 (3 μM; Figure 2B1). In these experiments, we used well-established characteristics to select dopaminergic neurons (Supporting Information Figure S1; see Methods for details). As reported and consistent with our results shown in Figure 1, the majority (~70%) of VTA neurons are dopaminergic neurons, with a small population of GABAergic neurons and glutamatergic neurons (Nair-Roberts *et al.*, 2008). Due to these considerations, the selection criteria and the subsequent confirmation by post-recording single-cell RT-PCR (see below), most of the recorded neurons were indeed dopaminergic neurons.

Fasudil induced a prominent increase in M-like currents in VTA dopaminergic neurons (Figure 2B1, C), with potency similar to that recorded in CHO cells overexpressing exogenous $K_v7.4$ channels (Figure 2B3). Deletion of $K_v7.4$ channels ($K_v7.4^{-/-}$ mice) greatly reduced the basal K_v7/M-like K^+ currents and completely abolished the effects of fasudil on K_v7/M-like K^+ currents in VTA dopaminergic neurons (Figure 2 B2, B3, C). These results strongly suggest that (i) fasudil selectively activates $K_v7.4$ channels and (ii) $K_v7.4$ channels are the functionally dominant K_v7 channel in VTA

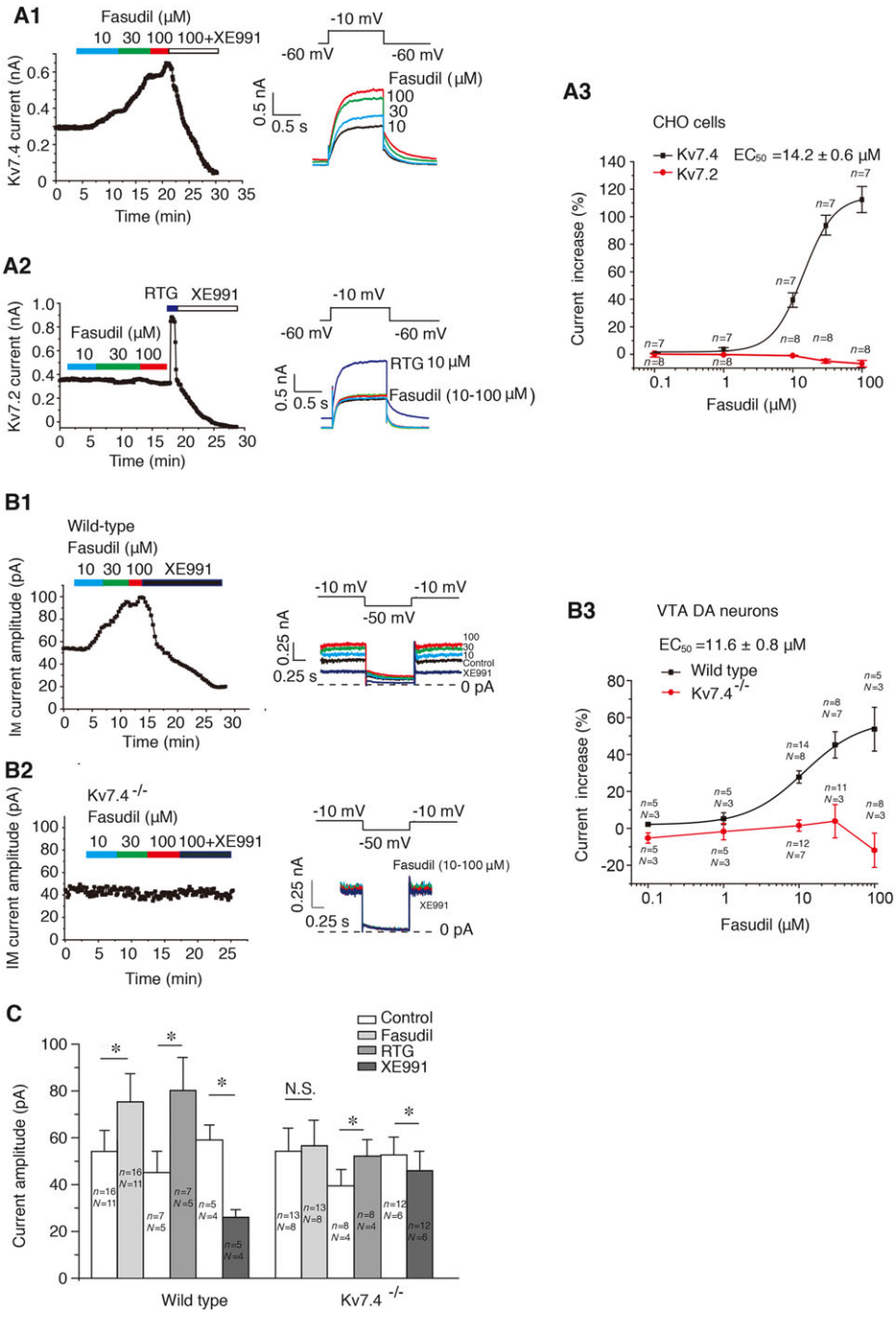

Figure 2

Fasudil selectively activates $K_v7.4$ channel currents in CHO cells and VTA dopaminergic neurons. Whole-cell patch clamp recordings from CHO cells and dopaminergic neurons in brain slices. (A1) Fasudil enhanced the currents of $K_v7.4$ channels stably expressed in CHO cells. The time course shown on the left is the time-lapsed deactivating tail current amplitudes recorded at −60 mV from a depolarizing steps to −10 mV in 20 s intervals. Typical current traces in the absence or presence of 10, 30 or 100 μM fasudil are shown on the right with the voltage pulse protocol shown in the inset above the traces. (A2) Fasudil (10, 30 or 100 μM) did not affect $K_v7.2$ channel currents, while retigabine (RTG; 10 μM) induced a threefold augmentation. (A3) Concentration–response curve for the effect of fasudil on $K_v7.4$ channel currents fitted with a logistic function; EC_{50} = 14.2 ± 0.6 μM. Fasudil had no detectable effect on the $K_v7.2$ currents. (B) K_v7/M currents recorded from VTA dopaminergic neurons from WT and $K_v7.4^{-/-}$ mice. (B1) shows the effects of fasudil (10, 30 or 100 μM) on the XE991-sensitive (3 μM) deactivating tail currents measured at −50 mV (left). The protocol used to induce K_v7/M currents and the corresponding current traces are shown in the right panel. (B3) The concentration–response relationships of the effect of fasudil on K_v7/M currents in dopaminergic neurons fitted with the logistic function; EC_{50} = 11.6 ± 0.8 μM. (C) The summarized effects of fasudil, retigabine and XE991 on K_v7/M current amplitude in VTA dopaminergic neurons from WT and $Kv7.4^{-/-}$ mice. *$P < 0.05$, significantly different as indicated; paired sample Wilcoxon signed ranks test for fasudil, paired *t*-test for XE991 and retigabine; *n* is the number of cells and *N* is the number of animals.

dopaminergic neurons. The residual small basal currents and the retigabine-activated currents in the $K_v7.4^{-/-}$ mice (Figure 2C) could arise from other K_v7 channels (Figure 1 A–C). We also tested the effects of fasudil on K_v7/M-like currents of SN dopaminergic neurons. In contrast to its effects in VTA dopaminergic neurons, fasudil did not induce significant activation of K_v7/M currents in SN neurons (from 94.1 ± 0.7 to 94.4 ± 0.2 pA after treatment with 100 μM fasudil; $n = 22$, $P > 0.05$, paired *t*-test).

$K_v7.4$ channel activity controls the excitability of VTA dopaminergic neurons

Next, we tested the influence of $K_v7.4$ channels on the excitability of VTA dopaminergic neurons. Excitability was recorded using a loose cell-attached patch method (Burlet *et al.,* 2002; Williams and Wozny, 2011) from brain slices of WT and $K_v7.4^{-/-}$ mice. We recorded from VTA neurons located primarily in the lateral part of the VTA, as projections from this population of VTA dopaminergic neurons are more likely to be involved in depression-like behaviour (Barbara and Han, 2016). The placement of recording electrodes and the positions of recorded neurons are shown in the schematic of Figure 3A2 (top). We recorded the spontaneous firing of VTA neurons with action potential wave form characteristics of dopaminergic neurons (Supporting Information Figure S1, Methods) (Figure 3A1, right panel). Fasudil (10 μM) significantly reduced the average firing frequency of VTA neurons (Figure 3A1, D). Post-recording single-cell PCR analysis confirmed that the inhibitory effect of fasudil resulted from activation of $K_v7.4$ channels, as fasudil only inhibited firing in VTA dopaminergic neurons that expressed these channels but did not inhibit firing in $K_v7.4$-negative neurons (Figure 3A2). The dopaminergic phenotype of these neurons was additionally confirmed by TH expression (Figure 3A2).

Fasudil did not affect the firing frequency in VTA dopaminergic neurons from $K_v7.4^{-/-}$ mice (Figure 3B, D). Consistent with the limited expression of $K_v7.4$ channels in the SN, the firing of dopaminergic neurons in the SN was not significantly affected by fasudil (Figure 3C, D). On the other hand, the firing of both VTA and SN neurons was inhibited by the non-selective K_v7 channel opener, retigabine and by a selective $K_v7.2$ channel opener RL-648-81 (10 μM; Kumar *et al.,* 2016) (Figure 3A–D). The effects of retigabine were still present in neurons from $K_v7.4^{-/-}$ mice (Figure 3B, D). These data support our finding that $K_v7.2$ channels are present in both VTA and SN neurons (Figure 1). In further evidence supporting a role of $K_v7.4$ channels in controlling DA neuron excitability, we found that the absence of $K_v7.4$ channels ($Kv7.4^{-/-}$) provides VTA dopaminergic neurons with a higher spontaneous firing frequency (Figure 3E). Furthermore, dopaminergic neurons in the SN of WT mice, which have limited expression of $K_v7.4$ channels, also had a higher firing frequency compared to VTA dopaminergic neurons from WT mice (Figure 3E). On the other hand, no difference in firing frequency between SN neurons from WT mice and $K_v7.4^{-/-}$ mice was found (Figure 3E).

We further tested the effects of K_v7 channel modulation on the excitability of VTA VTA dopaminergic neurons neurons using current-clamped, whole-cell recordings from VTA slices. In these experiments, the following parameters were recorded: (i) the resting membrane potential (Supporting Information Figure S4A); (ii) the induced action potential firing frequency (Supporting Information Figure S4B, C); and (iii) the spontaneous firing rates (Supporting Information Figure S4D). Comparison of these parameters between neurons fromWT and $K_v7.4^{-/-}$ mice clearly indicated that $K_v7.4$ channels constitutively modulated the excitability of VTA dopaminergic neurons.

Finally, the contribution of $K_v7.4$ channels to the regulation of excitability on VTA dopaminergic neurons was also assessed in an *in vivo* setting. The spontaneous firing of VTA dopaminergic neurons was recorded *in vivo* using an extracellular single-unit recording method (Figure 3F). In this recording paradigm, two patterns of firing (Figure 3F, expanded traces) were often recorded from the same neurons, the tonic firing (Figure 3F1) and burst firing (Figure 3F2; see Methods for detail), and both total firing frequency and the burst firing properties were analysed (Krishnan *et al.,* 2007). In WT mice, fasudil (i.p.; 20 mg·kg^{-1}) reduced the total firing frequency (Figure 3G1, G2) and the percentage of spikes in bursts (Figure 3G3) and increased the ISI (Figure 3G1). In marked contrast, in $K_v7.4^{-/-}$ mice, neither the total firing frequency nor the percentage of spikes in bursts was affected by fasudil treatment (Figure 3G2, G3).

The role of $K_v7.4$ channels in the development of a depression-like phenotype in the social defeat model of depression

Increased activity of VTA dopaminergic neurons is directly related to depression-like behaviours in the social defeat model of depression (Cao *et al.,* 2010; Chaudhury *et al.,* 2013; Friedman *et al.,* 2014.; Krishnan *et al.,* 2007). Because $K_v7.4$ channels play a significant role in controlling the excitability of VTA dopaminergic neurons, we investigated whether altered $K_v7.4$ channel activity could be a causal factor for the increased excitability of VTA dopaminergic neurons observed in the social defeat mice model. For this, we first established a model of social defeat (Figure 4A, Supporting Information Figure S2; see Methods for detail). The depression-like state of mice was confirmed by a reduction in sucrose preference (Figure 4B) and reduced social interaction time when an 'aggressor' CD1 mouse was present (Figure 4C). Mice that exhibited reduction in both parameters were defined as 'SUS mice'. Mice with both parameters unaltered were identified as 'UNSUS mice' (Krishnan *et al.,* 2007; Chaudhury *et al.,* 2013).

Consistent with the previous reports, the firing activity of VTA dopaminergic neurons, recorded using the *in vivo* single-unit recording method, was higher in SUS mice than in control and UNSUS mice (Figure 4D). Importantly, burst firing also increased in SUS mice compared to control and UNSUS mice (Figure 4E) and this increase has been reported to be an important determinant of depression-like behaviour in mice (Krishnan *et al.,* 2007; Chaudhury *et al.,* 2013).

We then recorded K_v7/M currents of VTA dopaminergic neurons from SUS and UNSUS mice. As shown in Figure 4F, K_v7/M currents were reduced in SUS mice compared with control and UNSUS mice (Figure 4). To test if the reduced K_v7/M currents were due to down-regulated expression of $K_v7.4$ channels, we first measured $K_v7.4$ mRNA levels using

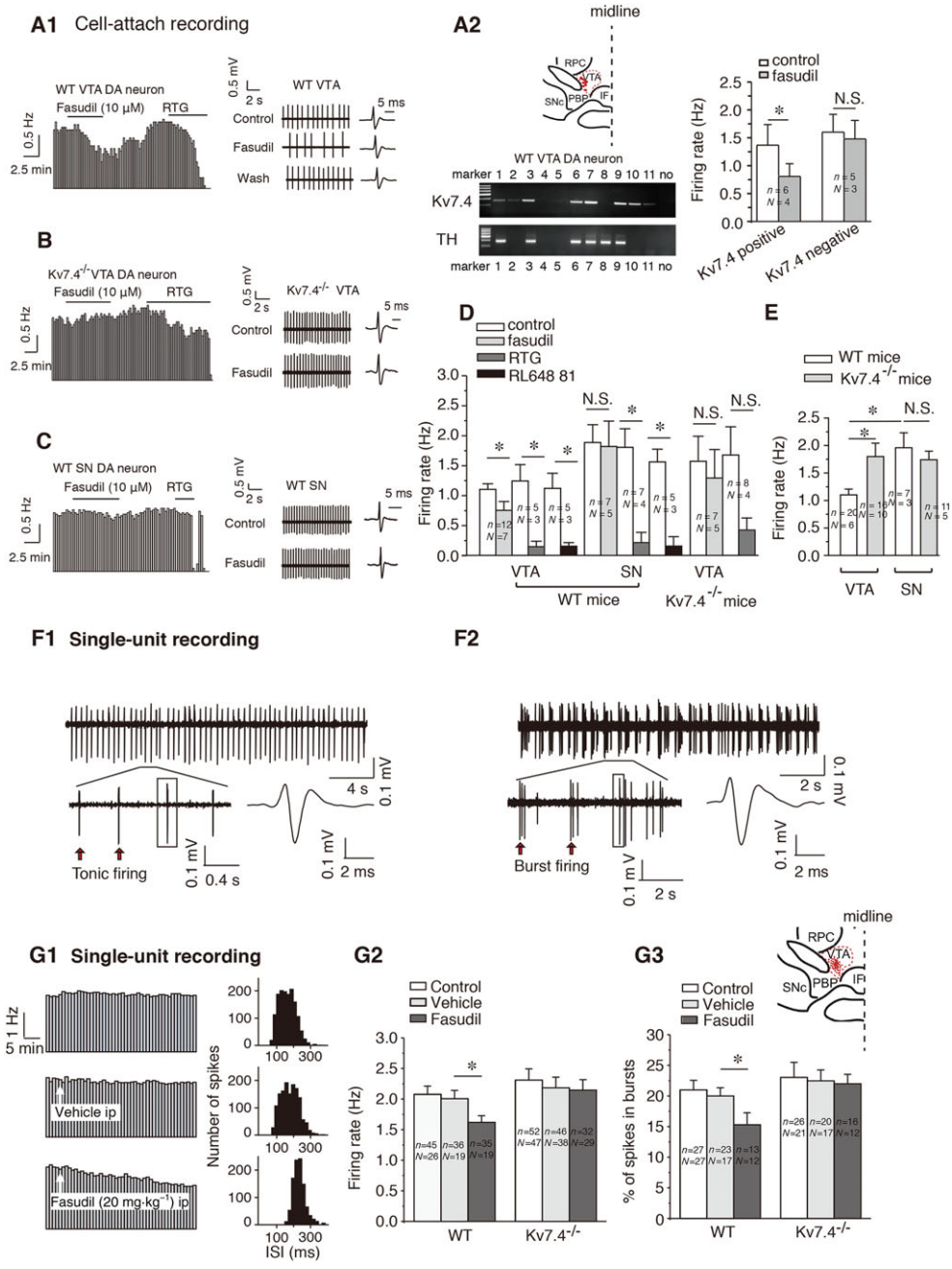

Figure 3

Fasudil decreases spontaneous firing of VTA dopaminergic neurons. (A–C) Cell-attached recording of spontaneous firing of dopaminergic neurons from VTA and SN areas. (A1) Effect of fasudil (10 μM) and retigabine (RTG; 10 μM) on the spontaneous firing frequency of VTA dopaminergic neurons from WT mice. Typical recordings and action potential waveforms are shown on the right. (A2) Left: Post-recording single-cell PCR shows the presence of $K_v7.4$ channels in TH-positive neurons. The inset on the top shows a map of a coronal midbrain slice indicating the location of neurons that were recorded and subsequently analysed with RT-PCR indicated (red dots). Right panel summarizes the effects of fasudil on the firing frequency of $K_v7.4$-positive and $K_v7.4$-negative, TH-expressing neurons. (B) Effect of fasudil and retigabine on spontaneous firing of VTA dopaminergic neurons from a $K_v7.4^{-/-}$ mouse. (C) Effect of fasudil and RTG on the spontaneous firing of SN DA neurons from a WT mouse. (D) Summary of the effects of fasudil, retigabine and a $K_v7.2$ channel selective activator, RL-648 81, on spontaneous firing frequency of VTA and SN dopaminergic neurons. *$P < 0.05$; N.S., not significant; paired *t*-test. (E) Summary of the spontaneous firing frequencies of VTA and SN dopaminergic neurons from WT and $K_v7.4^{-/-}$mice. (F) *In vivo* single-unit recording of spontaneously firing of VTA dopaminergicneurons. Examples of tonic (F1) and burst (F2) firing of dopaminergic neurons are shown. (G1) The time course of the firing frequency and the ISI of dopaminergic neurons following i.p. injection of fasudil (20 $mg \cdot kg^{-1}$) or vehicle (0.9% saline). The average firing frequency within 1 min bins is plotted against time. (G2) Summary of the effects of fasudil on the firing frequency recorded in experiments similar to those shown in G1. *$P < 0.05$, significantly different as indicated; one-way ANOVA. (G3) Summary of the effects of fasudil on the incidence of burst firing (percentage of spikes in bursts). *$P < 0.05$, significantly different as indicated; one-way ANOVA. *n* is the number of cells and *N* is the number of animals.

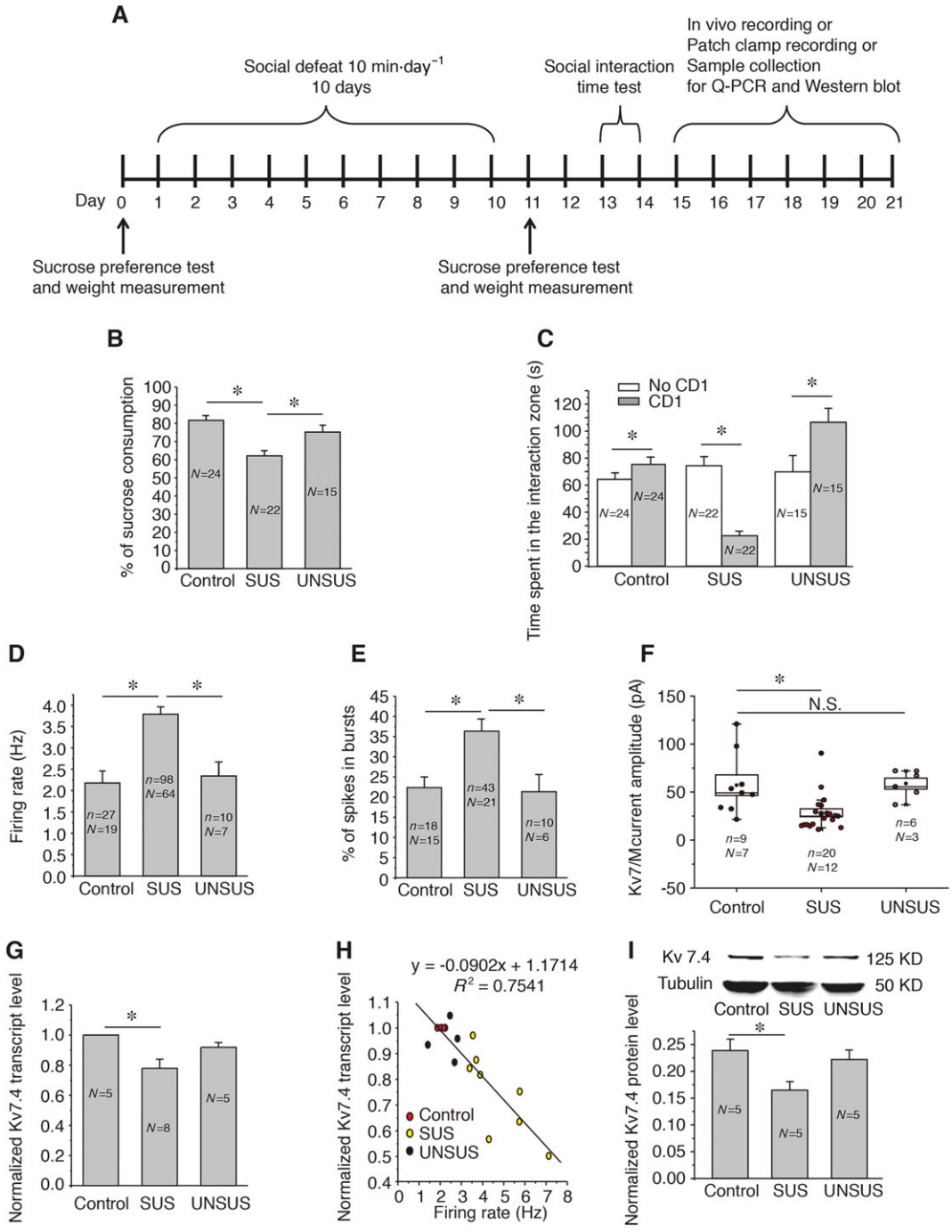

Figure 4

The role of $K_v7.4$ channels in the increased activity of VTA dopaminergic neurons in the social defeat model of depression. (A) Timeline of the chronic social defeat model. (B) The sucrose preference test. SUS, susceptible mice, UNSUS, unsusceptible mice (for detail, see Methods). *$P < 0.05$, significantly different as indicated; one-way ANOVA. (C) Social interaction test. The time that the test mice spent in the interaction zone in the absence ('No CD1') or presence ('CD1') of an unfamiliar CD1 mouse. *$P < 0.05$, significantly different as indicated; paired *t*-test. (D) Summary of firing frequencies of VTA dopaminergic neurons. Data from the *in vivo* single-unit recordings from control, SUS and UNSUS mice. (E) Percentage of spikes in bursts during the spontaneous firing of VTA dopaminergic neurons from control, SUS and UNSUS mice. *$P < 0.05$, significantly different as indicated; one-way ANOVA. (F) K_v7/M current amplitudes of VTA dopaminergic neurons from control, SUS and UNSUS mice, recorded using whole-cell patch clamp recording. N.S., not significant; Kruskal–Wallis ANOVA and Mann–Whitney test. (G) $K_v7.4$ mRNA expression measured with Q-PCR. *$P < 0.05$, significantly different as indicated; one-way ANOVA. (H) Correlation analysis of Kv7.4 mRNA levels and the firing frequency of the VTA dopaminergic neurons ($P < 0.05$; linear correlation analysis). The firing of VTA dopaminergic neurons was recorded using single-unit recording. Each point in the chart represents a result from a separate mouse. (I) $K_v7.4$ protein levels measured using Western blots. *$P < 0.05$, significantly different as indicated; one-way ANOVA; *n* is the number of cells and *N* is the number of animals.

qPCR. The results shown in Figure 4G demonstrated that the mRNA levels of $K_v7.4$ were indeed lower in the VTA of SUS mice compared with control and UNSUS mice. We also performed a correlation analysis and found that the firing frequency of VTA dopaminergic neurons was strongly negatively correlated with the expression level of $K_v7.4$ mRNA (R^2 = 0.75), regardless of the SUS/UNSUS phenotype (Figure 4H). We also measured the levels of $K_v7.4$ protein in the VTA and found that the abundance of this protein in the VTA of SUS mice was similarly reduced, Supporting Information Figure S7, compared with the levels in control and (to a lesser extent) UNSUS mice (Figure 4I), in good agreement with the RT-PCR data.

Fasudil reduces the excitability of VTA dopaminergic neurons and reverses depression-like behaviour

The results thus far allowed us to hypothesize that fasudil, by activating $K_v7.4$ channels in VTA dopaminergic neurons, should be able to ameliorate the increased excitability of VTA dopaminergic neurons and the related depression-like behaviour in a social defeat mouse model of depression. We used several approaches to test this hypothesis. First, we used the cell-attached recordings of the firing of VTA dopaminergic neurons from control, SUS and UNSUS mice. Indeed, fasudil reduced the firing rate of VTA dopaminergic neurons in SUS mice and control mice to similar extent (by about 30%) (Figure 5A1, A2). These results are consistent with reduced (but not abolished) expression of $K_v7.4$ channels and reduced M current amplitudes in the VTA DA neurons of SUS mice.

In further experiments, using *in vivo* single-unit recordings, we found that the total firing activity of dopaminergic neurons in the VTA of WT mice was decreased and that ISI increased significantly following i.p. injection of fasudil (20 mg·kg^{-1}) or retigabine (10 mg·kg^{-1}) but not vehicle (0.9% saline, 0.15 mL; Figure 5B, C). Similarly, burst firing was also decreased after treatment with fasudil and retigabine (Figure 5D, E). However, in $K_v7.4^{-/-}$ mice, fasudil failed to affect the firing of VTA dopaminergic neurons whereas retigabine remained effective, albeit with a reduced efficacy (Figure 5C).

Most importantly, the social defeat-induced avoidance behaviour of WT SUS mice was reversed by acute administration (i.p.) of fasudil and retigabine. Specifically, in vehicle-treated SUS mice, introduction of the unfamiliar CD1 mouse into the interaction test box (Supporting Information Figure S2B; Methods) induced an avoidance response from the tested mice. Thus, the time that the tested mice spent in the interaction zone was reduced (Figure 5F), indicating depression-like behaviour induced by social defeat. However, when WT SUS mice were injected with either retigabine or fasudil, the time that the tested mice spent in the interaction zone in the presence of the 'aggressor' CD1 mouse was not significantly different from the control period (without the 'aggressor'). This indicates that K_v7 channel openers indeed abolished the avoidance reaction to the introduction of the unfamiliar CD1 mice, indicating a reversal of depression-like social interaction deficit. It should be noted that when a CD1 mouse was absent, the time spent in the interaction zone for SUS mice from vehicle, fasudil or retigabine treatment groups (Figure 5F) was not significantly different. In $K_v7.4^{-/-}$ mice, however, fasudil failed to affect the behavioural response of SUS mice to the presence of the CD1 'aggressor' (Figure 5G). Retigabine however, was still effective (Figure 5G), but its effect was highly variable. Notably, under retigabine treatment, WT and $K_v7.4^{-/-}$ mice became less active, that is, their mobility in the open field test was significantly reduced (Supporting Information Figure S5B, C). This is consistent with the previously reported sedative effect of retigabine (Hayashi *et al.*, 2014). Fasudil, on the other hand, did not affect the general activity of the mice of either genotype (Supporting Information Figure S5B, C). These data suggest that retigabine, but not fasudil, exerts a central, sedative effect independent of $K_v7.4$ channels.

To provide direct evidence that fasudil, when administered systemically through i.p. injection, reversed the fault in social interaction of the social defeat mice through action on VTA dopaminergic neurons, fasudil was also infused directly onto the VTA through a cannula implanted to deliver at the VTA (Figure 6E, see Methods for details). Different concentrations of fasudil (and retigabine) were first tested to select a concentration of the drug to obtain an effect on the firing activity of dopaminergic neurons, comparable to that recorded after systemic administration. Ultimately, 200 μM was chosen to further test the effects of localized drug delivery on social interaction behaviour. At 200 μM, both fasudil and retigabine induced significant inhibition on VTA neuron firing activity (Figure 6A–C). Social interaction was tested at two time points after fasudil was administered, 5 and 40 min; a time-matched (5 min) vehicle control was also tested (Figure 6D). At both time points, local VTA infusion of fasudil or retigabine abolished 'aggressor' avoidance and normalized the time a mouse spent in the interaction zone (Figure 6F) and in the corner zone (Figure 6G) in the presence of a CD1 'aggressor'. Thus, as observed with systemic administration, direct local injection of fasudil into the VTA also reversed the depression-like social interaction behaviour.

Discussion

Here, we demonstrate that (i) $K_v7.4$ channels are selectively expressed in VTA dopaminergic neurons and represents a major K_v7/M channel in these cells; (ii) $K_v7.4$ channels play a key role in the regulation of the excitability of VTA dopaminergic neurons; (iii) down-regulation of $K_v7.4$ channels contributes importantly to the increased excitability of the VTA dopaminergic neurons and, thus, may trigger the development of a depression-like state in mice; and finally, (iv) fasudil is a selective opener of $K_v7.4$ channels, and its targeted modulation of these channels significantly improves depression-like behaviour in the social defeat mouse model of depression. As the excitability of VTA dopaminergic neurons is critical in the development of depressive state (Chaudhury *et al.*, 2013; Tye *et al.*, 2013), the $K_v7.4$ channels represent a promising target for developing new antidepressants. In this regard, our finding of selective activation of $K_v7.4$ channels and subsequent $K_v7.4$ channel-dependent reversal of a depression states by fasudil is particularly exciting. $K_v7.4$ channels have a much more restricted expression in the CNS compared to $K_v7.2$ and $K_v7.3$ channels (Hansen *et al.*, 2006; Hansen *et al.*,

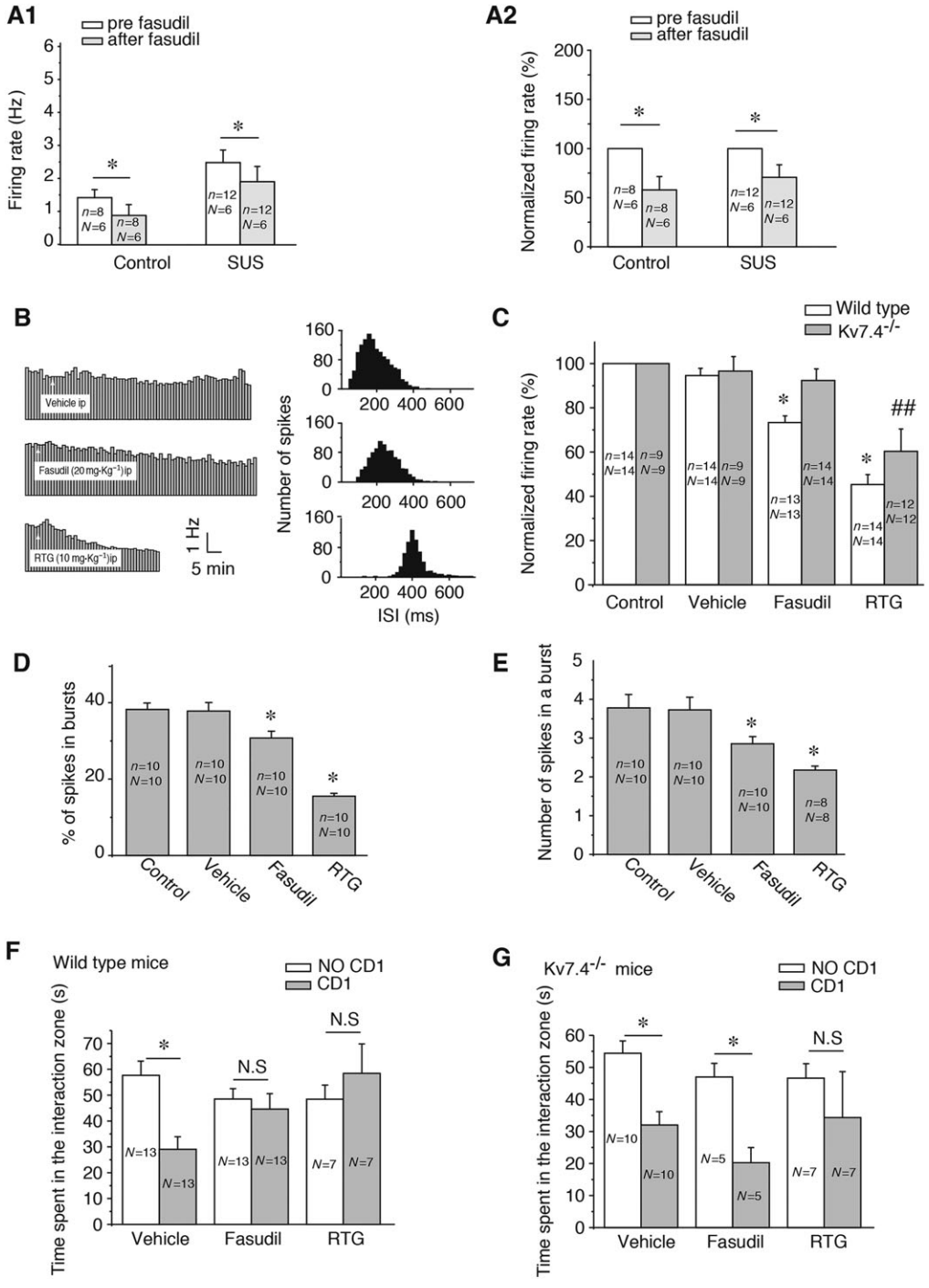

Figure 5

Fasudil reverses the depression-like behaviour in the mice developing social defeat through the activation of $K_v7.4$ channels. (A1) Effect of fasudil on the spontaneous firing rate of VTA dopaminergic neurons from control and SUS mice from cell-attached recording of dopaminergic neurons in VTA slices. *$P < 0.05$, significantly different as indicated; paired *t*-test. (A2) Normalized firing frequency based on the data shown in A1. *$P < 0.05$, significantly different as indicated; N.S., not significant; one sample Wilcoxon signed ranks test. (B) Effect of fasudil (20 mg·kg^{-1}, i.p.), retigabine (RTG; 10 mg·kg^{-1}, i.p.) or vehicle (0.9% saline) on the firing frequency and the ISI of VTA dopaminergic neurons recorded, using *in vivo* single-unit recording. The average firing frequency within 1 min bins is plotted against time. (C) Summary of the effect of fasudil and retigabine on the firing frequency of VTA dopaminergic neurons from WT and $K_v7.4^{-/-}$ mice. (D) Effect of fasudil and retigabine on the incidence of burst firing. *$P < 0.05$, significantly different as indicated; one-way ANOVA. (E) Effect of fasudil and retigabine on the number of spikes in a burst. *$P < 0.05$, significantly different as indicated; one-way ANOVA. (F) Effect of vehicle, fasudil and retigabine on the social interaction time of social defeat WT mice. N.S., not significant; paired *t*-test. (G) Effect of vehicle, fasudil and retigabine on the social interaction time of social defeat in $K_v7.4^{-/-}$ mice. N.S., not significant; paired *t*-test. *n* is the number of cells and *N* is the number of animals.

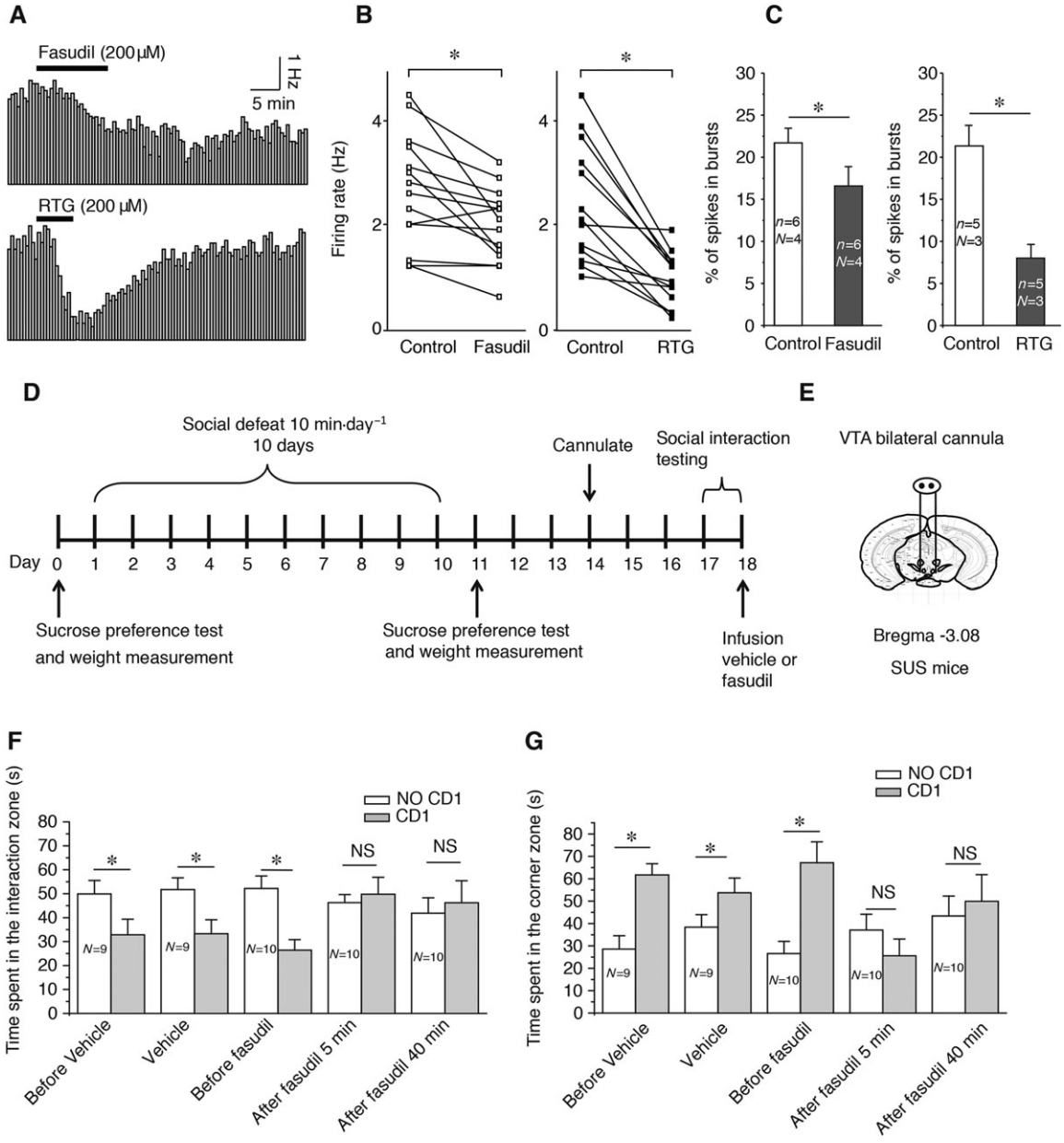

Figure 6

Microinfusion of fasudil into the VTA decreases the spontaneous firing of VTA DA neurons and reverses depression-like behaviour. (A) The time courses of the firing frequency of DA neurons following local injection of fasudil (200 μM; top) or RTG (200 μM; bottom) into the VTA of mice. (B) Summary of the effects of fasudil and RTG on the firing frequency recorded in experiments similar to those shown in A. (C) Summary of the effects of fasudil and RTG on the incidence of burst firing (percentage of spikes in bursts). (D) Timeline for the establishment of the social defeat model, the interaction test and the microinfusion of drugs. (E) Schematic depiction of cannula placement for direct microinjections of drugs into the VTA. (F, G) Summary of the effect of fasudil on social interaction: the time spent in the interaction zone (F) and in the corner zone (G). Tests were performed 5 and 40 min after the direct VTA infusion of fasudil (0.08 μg, 200 μM and 0.4 μL). N.S, not significant; paired *t*-test. *N* is the number of animals tested.

2008). This reduces the risk of on-target side effects of a selective $K_v7.4$ channel-based therapy, compared to broad-spectrum M channel targeting with currently available drugs such as retigabine. Consistent with this hypothesis, in our behavioural experiments, fasudil did not produce a sedative effect, while retigabine was clearly sedative (Supporting Information Figure S5). The fact that fasudil is already a clinically approved drug used for the treatment of cerebral vascular spasm (Uehata *et al.*, 1997) makes these findings even more relevant. Importantly, the anti-excitatory effects of fasudil in the VTA are likely to be independent of its **Rho kinase** inhibitor activity, as another unrelated Rho kinase inhibitor, Y-27632, did not affect the excitability of VTA dopaminergic neurons

recorded either *in vitro* or *in vivo* (Supporting Information Figure S6).

The argument that K^+ channel openers can be used to treat depression is based on the rationale that increased excitability of VTA dopaminergic neurons is linked to the development of depression, and thus, K^+ channel openers may help to reverse the over-excitable state of the VTA. The VTA activation theory is applicable to the social defeat depression model (Krishnan *et al.,* 2007; Cao *et al.,* 2010; Chaudhury *et al.,* 2013; Friedman *et al.,* 2014). In this model of depression, it is believed that increased phasic firing of VTA dopaminergic neurons *via* increased release of BDNF in the nucleus accumbens (NAc) confers individual susceptibility to stressful stimulation (Krishnan *et al.,* 2007; Chaudhury *et al.,* 2013). Elevated K^+ channel activity could counteract the increased VTA dopaminergic activity and alleviate depressive behaviour (Krishnan *et al.,* 2007; Friedman *et al.,* 2014; Friedman *et al.,* 2016). Thus, the VTA dopaminergic activation theory would involve the increased burst firing rates of VTA-NAc dopaminergic neurons as a crucial mediator of social stress-induced depressive behaviour (Walsh and Han, 2011). Our results conform well to this theory: the targeted activation of $K_v7.4$ channels reduced the increased excitability of VTA dopaminergic neurons and at the same time improved the depression-like behaviour of socially defeated mice. Importantly, the selective opener of $K_v7.4$ channels produced much fewer side effects compared to the broad-spectrum K_v7 channel opener retigabine.

The elevated neuronal excitability in VTA dopaminergic neurons from $K_v7.4^{-/-}$ mice might suggest a phenotype of depression. However, this was not the case; no depressive behaviour was observed in $K_v7.4^{-/-}$ mice and these mice developed depressive behaviour after being subjected to the stressful stimulation. This indicates that the elevated excitability of VTA neurons is essential, but not sufficient, for inducing the depression behaviour, and therefore, additional factors, such as corticotrophin release factor (Walsh and Han, 2011), may be necessary. Thus, a stress context is a precondition for the involvement of VTA dopaminergic neurons in the development of depressive behaviour (Chaudhury *et al.,* 2013).

The role of VTA dopaminergic neurons in the development of depression raises another question: could the reduced expression or activity of K^+ channels (including that of K_v7 channels induced, e.g. by stress) (Zhou *et al.,* 2016) be a causative factor in the altered firing of VTA dopaminergic neurons and the depression-like behaviours related to such altered firing? The results found thus far suggest that this may be the case. Earlier studies showed that elevated expression/activity of K^+ channels (including $K_v7.3$/KCNQ3) could be responsible for the lack of susceptibility in a subpopulation of mice that do not develop depression-like behaviour in the social defeat paradigm (Krishnan *et al.,* 2007; Friedman *et al.,* 2014; Friedman *et al.,* 2016). In the current study, we found that the mRNA and protein expression of $K_v7.4$ channels were lower in SUS mice, compared with those in UNSUS mice. Thus, our study suggests that the down-regulation of $K_v7.4$ channel abundance is possibly one of the causative factors of changes in the excitability of VTA dopaminergic neurons, which determines depressive behaviours (Chaudhury *et al.,* 2013; Tye *et al.,* 2013).

It has to be noted that our findings were obtained with the use of a single depression model. Different models of depression may involve different neuronal mechanisms, including the activity of VTA dopaminergic neurons (e.g. reduced activity of VTA dopaminergic neurons in the depression model of the unpredictable chronic mild stress, in mice; Chaudhury *et al.,* 2013; Tye *et al.,* 2013). This may underlie the complexity of major depressive states demonstrated in patients and their heterogeneous responses to antidepressants. Therefore, further studies are necessary to test if the mechanisms discovered here contribute to development of depression in other animal models and in patients. Nevertheless, targeting a causal molecular mechanism of depression (such as a loss of functional activity of $K_v7.4$ channels), rather than fighting symptoms of the disease, might provide a better strategy for development of new antidepressants.

In summary, in this study, we provide strong evidence that $K_v7.4$ channels are a key modulator of the excitability of VTA dopaminergic neurons, which contributes to the development of depressive behaviour. Furthermore, selective targeting of $K_v7.4$ channels in VTA dopaminergic neurons with drugs such as fasudil, presents a potential new strategy for the treatment of major depressive disorders.

Acknowledgements

This work was supported by the National Basic Research Program, Ministry of Science and Technology of the People's Republic of China (2013CB531302) and the National Natural Science Foundation of China (31270882) grants to H.Z., and Natural Sciences Fund of Shandong (ZR2013CQ033). We thank Han Hao for expert technical assistance.

Author contributions

H.Z. conceived and designed the experiments. L.L. and H.S. performed the experiments, acquired and analysed the data and prepared the figures. D.J. and C.N. performed behavior test, M.S. and L.Z. did electrophysiological test. Y.L. performed immunofluorescence of human brain slice. H.Z., N.G., X.D. and C.W. prepared the final version of the manuscript.

Conflict of interest

The authors declare no conflicts of interest.

Declaration of transparency and scientific rigour

This Declaration acknowledges that this paper adheres to the principles for transparent reporting and scientific rigour of preclinical research recommended by funding agencies,

publishers and other organisations engaged with supporting research.

References

Alexander SPH, Catterall WA, Kelly E, Marrion N, Peters JA, Benson HE *et al*. (2015a). The Concise Guide to PHARMACOLOGY 2015/16: Voltage-gated ion channels. Br J Pharmacol 172: 5904–5941.

Alexander SPH, Fabbro D, Kelly E, Marrion N, Peters JA, Benson HE *et al*. (2015b). The Concise Guide to PHARMACOLOGY 2015/16: Enzymes. Br J Pharmacol 172: 6024–6109.

Alexander SPH, Peters JA, Kelly E, Marrion N, Benson HE, Faccenda E *et al*. (2015c). The Concise Guide to PHARMACOLOGY 2015/16: Ligand-gated ion channels. Br J Pharmacol 172: 5870–5903.

Barbara J, Han MH (2016). Diversity of dopaminergic neural circuits in response to drug exposure. Neuropsychopharmacology 41: 2424–2446. https://doi.org/10.1038/npp.2016.32.

Borsotto M, Veyssiere J, Moha Ou Maati H, Devader C, Mazella J, Heurteaux C (2015). Targeting two-pore domain K(+) channels TREK-1 and TASK-3 for the treatment of depression: a new therapeutic concept. Br J Pharmacol 172: 771–784. https://doi.org/10.1111/bph.12953.

Brown DA, Passmore GM (2009). Neural KCNQ (Kv7) channels. Br J Pharmacol 156: 1185–1195. https://doi.org/10.1111/j.1476-5381.2009.00111.

Burlet S, Tyler CJ, Leonard CS (2002). Direct and indirect excitation of laterodorsal tegmental neurons by Hypocretin/Orexin peptides: implications for wakefulness and narcolepsy. J Neurosci 22: 2862–2872. https://doi.org/20026234.

Cao JL, Covington HE 3rd, Friedman AK, Wilkinson MB, Walsh JJ, Cooper DC *et al*. (2010). Mesolimbic dopamine neurons in the brain reward circuit mediate susceptibility to social defeat and antidepressant action. J Neurosci 30: 16453–16458. https://doi.org/10.1523/JNEUROSCI.3177-10.2010.

Chaudhury D, Walsh JJ, Friedman AK, Juarez B, Ku SM, Koo JW *et al*. (2013). Rapid regulation of depression-related behaviours by control of midbrain dopamine neurons. Nature 493: 532–536. https://doi.org/10.1038/nature11713.

Creed M, Kaufling J, Fois GR, Jalabert M, Yuan T, Lüscher C *et al*. (2016). Cocaine exposure enhances the activity of ventral tegmental area dopamine neurons via calcium-impermeable NMDARs. J Neurosci 36: 10759–10768. https://doi.org/10.1523/JNEUROSCI.1703-16.2016.

Curtis MJ, Bond RA, Spina D, Ahluwalia A, Alexander SPA, Giembycz MA *et al*. (2015). Experimental design and analysis and their reporting: new guidance for publication in BJP. Br J Pharmacol 172: 3461–3471. https://doi.org/10.1111/bph.12856.

Drion G, Bonjean M, Waroux O, Scuvee-Moreau J, Liegeois JF, Sejnowski TJ *et al*. (2010). M-type channels selectively control bursting in rat dopaminergic neurons. Eur J Neurosci 31: 827–835. https://doi.org/10.1111/j.1460-9568.2010.07107.x.

Dunlop BW, Nemeroff CB (2007). The role of dopamine in the pathophysiology of depression. Arch Gen Psychiatry 64: 327–337. https://doi.org/10.1001/archpsyc.64.3.327.

Franklin KBJ, Paxinos G (2001). The mouse brain: in stereotaxic coordinates. Academic Press: San Diego.

Friedman AK, Juarez B, Ku SM, Zhang H, Calizo RC, Walsh JJ *et al*. (2016). KCNQ channel openers reverse depressive symptoms via an active resilience mechanism. Nat Commun 24: 11671. https://doi.org/10.1038/ncomms11671.

Friedman AK, Walsh JJ, Juarez B, Ku SM, Chaudhury D, Wang J *et al*. (2014). Enhancing depression mechanisms in midbrain dopamine neurons achieves homeostatic resilience. Science 344: 313–319. https://doi.org/10.1126/science.1249240.

Gamper N, Shapiro MS. KCNQ Channels. (2015) In: Zheng J, Trudeau MC, Armstrong C, Hille B, Zagotta WN, Jan L, Catterall W, Hoshi T, Nichols CG, Goldstein SAN. Handbook of Ion Channels. CRC Press, Biophysics: Boca Raton, FL. pp 275–301

Gershon AA, Vishne T, Grunhaus L (2007). Dopamine D2-like receptors and the antidepressant response. Biol Psychiatry 61: 145–153. https://doi.org/10.1016/j.biopsych.2006.05.031.

Grace AA, Floresco SB, Goto Y, Lodge DJ (2007). Regulation of firing of dopaminergic neurons and control of goal-directed behaviours. Trends Neurosci 30: 220–227. https://doi.org/10.1016/j.tins.2007.03.003.

Hansen HH, Ebbesen C, Mathiesen C, Weikop P, Ronn LC, Waroux O *et al*. (2006). The KCNQ channel opener retigabine inhibits the activity of mesencephalic dopaminergic systems of the rat. J Pharmacol Exp Ther 318: 1006–1019. https://doi.org/10.1124/jpet.106.106757.

Hansen HH, Waroux O, Seutin V, Jentsch TJ, Aznar S, Mikkelsen JD (2008). Kv7 channels: interaction with dopaminergic and serotonergic neurotransmission in the CNS. J Physiol 586: 1823–1832. https://doi.org/10.1113/jphysiol.2007.149450.

Hayashi H, Iwata M, Tsuchimori N, Matsumoto T (2014). Activation of peripheral KCNQ channels attenuates inflammatory pain. Mol Pain 10: 15. https://doi.org/10.1186/1744-8069-10-15.

Heurteaux C, Lucas G, Guy N, El YM, Thümmler S, Peng XD *et al*. (2006). Deletion of the background potassium channel TREK-1 results in a depression-resistant phenotype. Nat Neurosci 9: 1134–1141. https://doi.org/10.1038/nn1749.

Jentsch TJ (2000). Neuronal KCNQ potassium channels: physiology and role in disease. Nat Rev Neurosci 1: 21–30. https://doi.org/10.1038/35036198.

Kharkovets T, Dedek K, Maier H, Schweizer M, Khimich D, Nouvian R *et al*. (2006). Mice with altered KCNQ4 K+ channels implicate sensory outer hair cells in human progressive deafness. EMBO J 25: 642–652. https://doi.org/10.1038/sj.emboj.7600951.

Kilkenny C, Browne W, Cuthill IC, Emerson M, Altman DG (2010). Animal research: reporting *in vivo* experiments: the ARRIVE guidelines. Br J Pharmacol 160: 1577–1579.

Koyama S, Appel SB (2006). Characterization of M-current in ventral tegmental area dopamine neurons. J Neurophysiol 96: 535–543. https://doi.org/10.1152/jn.00574.2005.

Krishnan V, Han MH, Graham DL, Berton O, Renthal W, Russo SJ *et al*. (2007). Molecular adaptations underlying susceptibility and resistance to social defeat in brain reward regions. Cell 131: 391–404. https://doi.org/10.1016/j.cell.2007.09.018.

Kumar M, Reed N, Liu R, Aizenman E, Wipf P, Tzounopoulos T (2016). Synthesis and evaluation of potent KCNQ2/3-specific channel activators. Mol Pharmacol . https://doi.org/10.1124/mol.115.103200.

Mameli-Engvall M, Evrard A, Pons S, Maskos U, Svensson TH, Changeux JP *et al*. (2006). Hierarchical control of dopamine neuron-

firing patterns by nicotinic receptors. Neuron 50: 911–921. https://doi.org/10.1523/JNEUROSCI.1958-08.2008.

Mazella J, Petrault O, Lucas G, Deval E, Beraud-Dufour S, Gandin C *et al*. (2010). Spadin, a sortilin-derived peptide, targeting rodent TREK-1 channels: a new concept in the antidepressant drug design. PLoS Biol 8 e1000355. doi:https://doi.org/10.1371/journal.pbio.1000355.

McGrath JC, Lilley E (2015). Implementing guidelines on reporting research using animals (ARRIVE etc.): new requirements for publication in BJP. Br J Pharmacol 172: 3189–3193. https://doi.org/10.1111/bph.12955.

Munoz MB, Slesinger PA (2004). Sorting nexin 27 regulation of G protein-gated inwardly rectifying K(+) channels attenuates in vivo cocaine response. Neuron 82: 659–669. https://doi.org/10.1016/j.neuron.2014.03.011.

Nair-Roberts RG, Chatelain-Badie SD, Benson E, White-Cooper H, Bolam JP, Ungless MA (2008). Stereological estimates of dopaminergic, GABAergic and glutamatergic neurons in the ventral tegmental area, substantia nigra and retrorubral field in the rat. Neuroscience 152: 1024–1031. https://doi.org/10.1016/j.neuroscience.2008.01.046.

Neuhoff H, Neu A, Liss B, Roeper J (2002). I(h) channels contribute to the different functional properties of identified dopaminergic subpopulations in the midbrain. J Neurosci 22: 1290–1302 doi:22/4/1290 [pii].

Overstreet DH, Wegener G (2013). The flinders sensitive line rat model of depression – 25 years and still producing. Pharmacol Rev 65: 143–155. https://doi.org/10.1124/pr.111.005397.

Padgett C, Lalive A, Tan K, Terunuma M, Munoz M, Pangalos M *et al*. (2012). Methamphetamine-evoked depression of GABA B receptor signaling in GABA neurons of the VTA. Neuron 73: 978–989. https://doi.org/10.1016/j.neuron.2011.12.031.

Schultz W (2007). Multiple dopamine functions at different time courses. Annu Rev Neurosci 30: 259–288. https://doi.org/10.1146/annurev.neuro.28.061604.135722.

Shabat-Simon M, Levy D, Amir A, Rehavi M, Zangen A (2008). Dissociation between rewarding and psychomotor effects of opiates: differential roles for glutamate receptors within anterior and posterior portions of the ventral tegmental area. J Neurosci 28: 8406–8416. https://doi.org/10.1523/JNEUROSCI.1958-08.2008.

Southan C, Sharman JL, Benson HE, Faccenda E, Pawson AJ, Alexander SPH *et al*. (2016). The IUPHAR/BPS guide to PHARMACOLOGY in 2016: towards curated quantitative interactions between 1300 protein targets and 6000 ligands. Nucl Acids Res 44: D1054–D1068.

Tatulian L, Delmas P, Abogadie FC, Brown DA (2001). Activation of expressed KCNQ potassium currents and native neuronal M-type potassium currents by the anti-convulsant drug retigabine. J Neurosci 21: 5535–5545 doi:21/15/5535 [pii].

Tsai HC, Zhang F, Adamantidis A, Stuber GD, Bonci A, de Lecea L *et al*. (2009). Phasic firing in dopaminergic neurons is sufficient for behavioural conditioning. Science 324: 1080–1084. https://doi.org/10.1126/science.1168878.

Tye KM, Mirzabekov JJ, Warden MR, Ferenczi EA, Tsai HC, Finkelstein J *et al*. (2013). Dopamine neurons modulate neural encoding and expression of depression-related behaviour. Nature 493: 537–541. https://doi.org/10.1038/nature11740.

Uehata M, Ishizaki T, Satoh H, Ono T, Kawahara T, Morishita T *et al*. (1997). Calcium sensitization of smooth muscle mediated by a Rho-associated protein kinase in hypertension. Nature 389: 990–994. https://doi.org/10.1038/40187.

Ungless MA, Magill PJ, Bolam JP (2004). Uniform inhibition of dopamine neurons in the ventral tegmental area by aversive stimuli. Science 303: 2040–2042. https://doi.org/10.1126/science.1093360.

Veyssiere J, Moha Ou Maati H, Mazella J, Gaudriault G, Moreno S, Heurteaux C *et al*. (2015). Retroinverso analogs of spadin display increased antidepressant effects. Psychopharmacology (Berl) 232: 561–574. https://doi.org/10.1007/s00213-014-3683-2.

Walsh JJ, Han MH (2011). The heterogeneity of ventral tegmental area neurons: projection functions in a mood-related context. Neuroscience 282C: 101–108. https://doi.org/10.1016/j.neuroscience.2014.06.006.

Wang HS, Pan Z, Shi W, Brown BS, Wymore RS, Cohen IS *et al*. (1998). KCNQ2 and KCNQ3 potassium channel subunits: molecular correlates of the M-channel. Science 282: 1890–1893. https://doi.org/10.1126/science.282.5395.1890.

Williams SR, Wozny C (2011). Errors in the measurement of voltage-activated ion channels in cell-attached patch-clamp recordings. Nat Commun 2: 242. https://doi.org/10.1038/ncomms1225.

Wong ML, Licinio J (2001). Research and treatment approaches to depression. Nat Rev Neurosci 2: 343–351. https://doi.org/10.1038/35072566.

Zhang X, An H, Li J, Zhang Y, Liu Y, Jia Z *et al*. (2016). Selective activation of vascular $K_v7.4/K_v7.5$ K+ channels by fasudil contributes to its vasorelaxant effect. Br J Pharmacol . https://doi.org/10.1111/bph.13639.

Zhou JJ, Gao Y, Kosten TA, Zhao Z, Li DP (2016). Acute stress diminishes M-current contributing to elevated activity of hypothalamic-pituitary-adrenal axis. Neuropharmacology 114: 67–76. https://doi.org/10.1016/j.neuropharm.2016.11.024.

Supporting Information

Additional Supporting Information may be found online in the supporting information tab for this article.

https://doi.org/10.1111/bph.14026

Figure S1 Electrophysiological identification of VTA DA neurons. (A) Current-clamp recording from a VTA DA neuron showing Ih-mediated sag response to the injection of −300 pA hyperpolarizing current. (B) Summarized data for the peak amplitude of sag potential shown in A. No difference was found between the VTA DA neurons from WT and Kv7.4$^{-/-}$ mice ($P > 0.05$; unpaired t-test). (C) and (D) Characteristic DA neuron action potential (AP) waveform; (C1) Example AP recorded from a DA neurons in VTA slice using loosely cell-attached patch recording; dotted lines represent the margins of the AP width (as measured from the onset to the negative deflection peak) which are considered characteristic of a DA neuron. (C2) Summarized AP duration for putative DA neurons from WT and Kv7.4$^{-/-}$ mice. Panels D1-D2 are similar to C1-C2 but dotted lines now represent the AP width as measured from the onset to the end of negative deflection; this parameter was set at >2.5 ms for a neuron to be considered a DA neuron. For panels C2 and D2 $P > 0.05$, unpaired t-test. n is the number of cells and N is the number of animals.
Figure S2 Social interaction test for the social defeat model of depression. (A) Typical locomotor activity traces of

control, susceptible (SUS) and unsusceptible (UNSUS) mice in a social interaction test box (schematically shown in panel B) in the absence (blank) and presence (mouse image) of an unfamiliar CD1 mouse. (B) Schematic top-down view of the social interaction arena. (C) Time the tested control, SUS and UNSUS mice spent in the corner zones of the social interaction arena.

Figure S3 Effect of fasudil on Kv7.2/7.3 currents in CHO cells. A. and B. Time course (A) and example traces (B) showing effect of fasudil (10 μM, 30 μM or 100 μM) and RTG (10 μM) on currents of Kv7.2/Kv7.3 heteromers expressed in CHO cells. (C) Effect of multiple concentrations (0.1–100 μM) of fasudil and a single concentration of RTG (10 μM) on Kv7.2/Kv7.3 currents. No effect of fasudil was observed while RTG increased KV7.2/Kv7.3 currents by 234.7 ± 25.8%. The deactivating currents at −60 mV were recorded using the protocol shown at the top of panel B. n is the number of cells.

Figure S4 Effects of fasudil on the resting membrane potential and the elicited action potential spikes of VTA DA neurons. (A) Summarized effects of 10 μM fasudil and 3 μM XE991 on the resting membrane potential (RMP) of VTA DA neurons from wild type and $Kv7.4^{-/-}$ mice recorded using the whole-cell current-clamp technique. N.S, not significant, paired t-test. (B) and (C) Effects of fasudil on the action potential firing induced by injection of depolarizing currents in WT mice and $Kv7.4^{-/-}$ mice. (B1) and (C1) Example traces obtained with 150 pA current injection in VTA DA neurons from WT (B1) and $Kv7.4^{-/-}$ (C1) mice respectively. (B2) Summary of the effects of fasudil on spike number of DA neurons from WT mice; firing was induced by incremental current injections (50, 100, 150, and 200 pA). *$P < 0.05$, paired t-test. (C2) Similar to B2 but recordings were performed from DA neurons from $Kv7.4^{-/-}$ mice. N.S., not significant; paired t-test. n is the number of cells and N is the number of animals. (D1) Effect of fasudil on spontaneous firing of DA neurons from wild type and $K_v7.4^{-/-}$ mice recorded using whole-cell patch clamp recording technique. (D2) Summary of the fasudil effect (10 μM at 10 min of continuous application) for D1. *$P < 0.05$, N.S., not significant, paired t-test.

Figure S5 Effects of Kv7 openers on the general locomotor activity of mice in the open field test. (A) Timeline of drug administration and social interaction test. Vehicle (0.9% saline), fasudil (20 $mg{\cdot}kg^{-1}$) and RTG (10 $mg{\cdot}kg^{-1}$) were given intraperitoneally (i.p.) to the control or SUS mice. 10 min after drugs administration, the mice were subjected to the social interaction test. (B) Summarized data for locomotor activity of WT mice under influence of RTG (10 $mg{\cdot}kg^{-1}$, i.p.) and fasudil (20 $mg{\cdot}kg^{-1}$, i.p.) in the open field test. (C) Summarized data for locomotor activity of $Kv7.4^{-/-}$ mice under influence of RTG (10 $mg{\cdot}kg^{-1}$, i.p.) and fasudil (20 $mg{\cdot}kg^{-1}$, i.p.) in the open field test. N is the number of animals.

Figure S6 Effect of Rho kinase inhibitor Y-27632 on the spontaneous firing of VTA DA neurons. (A) The time course of the firing frequency of a DA neuron recorded using the *in vivo* single unit recording technique, following local injection of Rho kinase inhibitor Y-27632 (200 μM) into VTA of a mouse. (B) Summary of the effect of Y-27632 for experiments shown in A. N.S., not significant, paired t-test. (C) Effect of Y-27632 (10 μM) on spontaneous firing of VTA DA neurons recorded using the *in vitro* cell-attached recording technique from on a VTA brain slice. (D) Summary of the effect of Y-27632 for experiments shown in C. N.S. not significant, paired t-test. n is the number of cells and N is the number of animals.

Figure S7 Kv7.4 protein levels from VTA samples of control, suseptible and unsuseptible mice measured using western blot.